1   ## *In vivo* Imaging β-cell Function Reveals Two Waves of β-cell Maturation

2   Jia Zhao[1], Weijian Zong[1,5], Yi Wu[4], Jiayu Shen[1], Dongzhou Gou[1], Yiwen Zhao[1], Runlong Wu[3], Fuzeng

3   Niu[2], Xu Wang[1], Xuan Zheng[1], Aimin Wang[2], Yunfeng Zhang[3], Jing-Wei Xiong[1], Liangyi Chen[1*], Yanmei

4   Liu[1*]

5

6   **Affiliations:**

7   [1]State Key Laboratory of Membrane Biology, Beijing Key Laboratory of Cardiometabolic Molecular

8   Medicine, Institute of Molecular Medicine, Peking University, Beijing 100871, China

9   [2]State Key Laboratory of Advanced Optical Communication System and Networks, School of Electronics

10   Engineering and Computer Science, Peking University, Beijing 100871, China

11   [3]School of Electronics Engineering and Computer Science, Peking University, Beijing 100871, China

12   [4]School of Software and Microelectronics, Peking University, Beijing 100871, China

13   [5]China Department of Cognitive Sciences, Institute of Basic Medical Sciences, Beijing 100850, China

14   *Correspondence: yanmeiliu@pku.edu.cn; lychen@pku.edu.cn

15

16

Abstract

The insulin-secreting cells generated from stem cells *in vitro* are less glucose responsive than primary β-cells. To search for the missing ingredients that are needed for β-cell maturation, we have longitudinally monitored function of every β-cell in Tg *(ins:Rcamp1.07)* zebrafish embryos with a newly-invented two-photon light-sheet microscope. We have shown that β-cell maturation begins from the islet mantle and propagates to the islet core during the hatching period, coordinated by the islet vascularization. Lower concentration of glucose is optimal to initiate β-cell maturation, while increased glucose delivery to every cell through microcirculation is required for functional boosting of the β-cells. Both the initiation and the boosting of β-cell maturation demands activation of calcineurin/NFAT by glucose. Calcineurin activator combined with glucose promotes mouse neonatal β-cells cultured *in vitro* to mature to a functional state similar to adult β-cells, suggesting a new strategy for improving stem cell-derived β-like cell function *in vitro*.

Keywords

functional maturation of β-cells *in vivo*; ins:Rcamp1.07 zebrafish, 2P3A-DSLM; microcirculation; glucose.

Introduction

44

45 Pancreatic β-cells secrete insulin to regulate blood glucose metabolism. An insufficient functional β-

46 cell mass causes glucose intolerance and diabetes. To generate new therapeutic approaches for diabetes, β-

47 cell development has been intensively studied during the last two decades. While much has been understood

48 regarding the early development of pancreatic progenitor cells (Pan & Wright, 2011), the mechanisms

49 regarding the final β-cell maturation are still poorly defined (Kushner et al, 2014). β-cells reside in islets

50 that consist of endocrine, vascular, neuronal and mesenchymal cells. Various cues arising from this

51 neurovascular milieu, such as gap junctions, neuronal transmitters, endothelial factors and hormones, have

52 been reported to be involved in β-cell development (Borden et al, 2013; Carvalho et al, 2010; Cleaver &

53 Dor, 2012; Omar et al, 2016). The absence of these factors from the culture media that is used by current *in*

54 *vitro* differentiation protocols may account for the limited glucose-responsiveness of stem cell-derived β-

55 like cells (Bruin et al, 2015; Rezania et al, 2014). Hence, knowing how pancreatic β-cells mature *in*

56 *situ* during development may guide the addition of key factors to the culture medium to promote the final

57 maturation of β-like cells *in vitro*.

58 A major difficulty in studying β-cell maturity *in vivo* with traditional methods is to evaluate β-cell

59 function independent of β-cell mass. Imaging function of individual β-cells will overcome this problem.

60 The primary function of a mature β-cell is to quickly secrete the stored insulin in responding to increases

61 of blood glucose concentration. Glucose-triggered Ca^{2+} influx in pancreatic β-cells is essential for the

62 insulin secretion, thus often serves as a functional marker to evaluate β-cell maturity in living organisms

63 (Pagliuca et al, 2014; Rezania et al, 2014). Ca^{2+} transient in primary β-cells can be imaged in isolated islets

64 when β-cells are labelled with genetically encoded fluorescent Ca^{2+} indicators. However, to image Ca^{2+}

65 transients in β-cells *in vivo* noninvasively remains the unmet challenge due to the non-transparency of the

66 pancreas tissues in mammals.

67 Here we used zebrafish as the model animal in which β-cell development is conserved with mammals

68 and their maturation processes can be observed in the transparent, externally developed embryos of

69 zebrafish (Huang et al, 2001). With every β-cell labelled with Rcamp1.07, a red fluorescent Ca^{2+} indicator

70   in Tg (*ins:Rcamp1.07*) zebrafish, we use our newly developed high-resolution two-photon three-axis digital

71   scanning light-sheet microscope (2P3A-DSLM) to visualize glucose-stimulated Ca^{2+} responses in

72   individual β-cells *in vivo*. The first glucose-responsive β-cells appear from the islet mantle at 48 hours post-

73   fertilization (hpf). Based on the Ca^{2+} transient kinetics, we characterized the glucose-responsive β-cells into

74   two stages: the initiation and the boosting of the maturation. This early β-cell maturation of the islet mantle

75   requires low local glucose concentration and is independent of vascularization. With islet vascularization

76   from 60 hpf to 72 hpf, increased glucose concentration delivered through islet microcirculation, initiates β-

77   cell maturation in the islet core and pushes all glucose-responsive β-cells towards further maturity. By

78   manipulating with inhibitors, activators and the dominant negative mutant, we demonstrate that the

79   calcineurin/NFAT signaling pathway acts downstream of glucose to initiate, boost and sustain β-cells

80   maturation. Finally, we showed that neonatal mouse β-cells within isolated islets can be promoted towards

81   optimal maturity *in vitro* by the combination of a calcineurin activator and glucose, demonstrating that

82   mammalian β-cell maturation shares the conserved mechanism. This data also highlights the practicality of

83   direct activation of calcineurin/NFAT in pushing stem cell-derived β-like cells towards optimal maturity *in*

84   *vitro*.

85

Results

Visualization of β-cell maturation in vivo with 2P3A-DSLM

To visualize β-cell function, we created a transgenic zebrafish line, Tg (*ins:Rcamp1.07*), in which the red fluorescent calcium indicator Rcamp1.07 (Ohkura et al, 2012) is under the control of the insulin promoter. Rcamp1.07 is expressed exclusively in β-cells, as confirmed by the cellular co-localization of Rcamp1.07 with EGFP in Tg (*ins:Rcamp1.07*)*;* Tg (*ins:EGFP*) double transgenic fish (Huang et al, 2001) (Figure 1-Figure Supplement 1A-F) and with immunofluorescently labelled insulin in Tg (*ins:Rcamp1.07*) fish (Figure 1-Figure Supplement 1G-J). Within 5 min after stimulating live 72 hpf Tg (*ins:Rcamp1.07*) fish embryos with 20 mM glucose, we observed a robust transient increase in the fluorescence intensity of Rcamp1.07 under a wide-field microscope (Figure 1-Figure Supplement 2 and Supplemental Movie 1), indicative of the glucose-stimulated Ca^{2+} transients *in vivo*. However, individual β-cells are hardly discernible under the wide-field (Figure 1-Figure Supplement 2) or a single-photon selective-plane illuminative microscope (1P-SPIM) (Figure 1-Figure Supplement 2). With a two-photon microscope (TPM), we could resolve individual β-cells in the XY plane, but the cell boundaries along Z-axis were blurred due to the low axial resolution and high scattering of the illumination light in deep tissues. Only with our newly-developed 2P3A-DSLM (Supplemental Movie 2), we could reconstruct a clear three-dimensional structure of the islet in live fish embryos (Figure 1A and B, Supplemental Movie 2 and Supplemental Movie 3). To our knowledge, this is the first time to achieve high-resolution *in vivo* imaging of individual β-cells and their functions.

By counting insulin-positive cells and glucose-responsive β-cells at different stages of Tg (*ins:Rcamp1.07*); Tg (*ins:EGFP*) fish embryos, we identified a proliferation of β-cells during 36-48 hpf, followed by a progressive increase in glucose-responsive β-cells during the hatching period (Figure 1C and Figure 1-Figure Supplement 3A). Along with the increase of glucose-responsive β-cells, mature β-cell marker MafA positive β-cells also increased (Figure 1D and E), indicating that by counting glucose-responsive β-cells we could evaluate the *bona fide* maturation process of β-cells. Because the speed (time to rise) and the maximal amplitude (Max ΔF/F) of the glucose-stimulated Ca^{2+} transients are key parameters

112   of β-cell functionality (Bruin et al, 2015; Rezania et al, 2014), we used them as criteria to evaluate the

113   maturity levels of individual β-cells *in vivo* (Figure 1-Figure Supplement 3B). The first glucose-responsive

114   β-cell appeared at 48 hpf and we defined it to be at the initiation stage of maturation. Compared to glucose-

115   responsive β-cells at 48 hpf, the cells at 56 hpf exhibited faster and larger Ca^{2+} responses evoked by glucose

116   stimulation on average as many cells have entered the function boosting stage. These average responses

117   were further accelerated and enhanced at 72 hpf, when β-cells responded within ~ 90 s of glucose

118   administration with a ~150% of the maximal amplitude of the evoked Ca^{2+} transient (Figure 1 F and G and

119   Figure 1-Figure Supplement 3C and D). Therefore, with our β-cell-function visualization zebrafish system,

120   we observed a gradual maturation process of β-cells *in vivo* from 48 to 72 hpf.

121

122   ***Sequential maturation of β-cells from the islet mantle to the core is coordinated with islet vascularization***

123   Next, we investigated whether islet vascularization affect β-cell maturation *in vivo* by labelling both β-cells

124   and vascular endothelial cells in Tg (*ins:EGFP*); Tg (*flk1:mCherry*) fish (Wang et al, 2013). We found that

125   blood vessels initiated contacts with the islet mantle from 48 to 60 hpf and further penetrated into the inner

126   layers of the islet from 60 to 72 hpf (Figure 2A and Supplemental Movie 4). Most of the glucose-responsive

127   β-cells was proximal to blood vessels (Figure 2-Figure Supplement 1A), and their longitudinal increase

128   was paralleled with the increase of β-cells adjacent to the vessels (Figure 2B and Figure 2-Figure

129   Supplement 1B).

130   As islet vascularization progressed from the mantle to the core, we then examined whether β-cells in

131   the mantle and β-cells in the core matured differently during development (Figure 2C). From 48 to 60 hpf,

132   β-cells in the mantle acquired function earlier than those in the core, with more glucose-responsive β-cells

133   (Figure 2D), higher maximum Ca^{2+} transients (Figure 2E) and faster responses (Figure 2F). Only during the

134   late hatching period did β-cells in the core start to mature at an accelerated pace. At 72 hpf, they were

135   indistinguishable from β-cells in the mantle in terms of all related parameters (Figure 2D-F). Therefore, β-

136   cells in the mantle mature differently from those in the core both in the initiation time window and function

137   boosting dynamics.

138   To explore whether the heterogeneous maturation process is caused by islet vascularization, we

139   examined β-cell maturation in Tg(*ins:Rcamp1.07*) *cloche* mutant embryos, which have no vascular

140   endothelial cells or blood cells but a normal number of β-cells (Figure 2G and Figure 2-Figure Supplement

141   1C) (Field et al, 2003a). Glucose-responsive β-cells in 56 hpf *cloche* embryos were indistinguishable from

142   those in age-matched controls (Figure 2H and I). At 72 hpf, in contrast, *cloche* mutants had fewer glucose-

143   responsive β-cells in the islet core and exhibited smaller maximum Ca^{2+} transients in responding β-cells

144   than the controls (Figure 2H and I). Without islet microcirculation, β-cells of *cloche* mutants stayed in a

145   maturation state similar to that in 60 hpf control embryos (Figure 3-Figure Supplement 1). Therefore, β-

146   cells mature in two waves *in vivo*: first, mantle β-cells acquire glucose responsiveness independent of islet

147   vascularization during 48-60 hpf; next, islet vascularization initiates the maturation of the β-cells in the islet

148   core and promotes all glucose-responsive β-cells to further mature during 60-72 hpf. To test whether blood

149   circulation or endothelial cells provide the key inductive factor, we stopped the blood circulation with 2,3-

150   butanedione monoxime (2,3-BDM) (Bartman et al, 2004) for 9 hours in *ins:Rcamp1.07* embryos at either

151   the early or the late hatching period. Despite intact islet vascularization after the circulation blockade (data

152   not shown), 2,3-BDM treatment inhibited β-cell maturation to a similar extent as that of *cloche* mutants

153   (Figure 2H and I). Therefore, blood circulation *per se*, but not endothelial cells, provides the key inductive

154   signal for β-cells in the islet core to initiate and further promote their maturation.

155

156   ***Increased glucose delivered by the microcirculation controls sequential β-cell maturation***

157   Glucose, the major nutrient in the circulation system, is known to regulate embryonic pancreatic endocrine

158   cell differentiation *in vitro* (Guillemain et al, 2007). To explore whether glucose could be the inductive

159   signal for β-cell maturation, we used 3-mercaptopicolinic acid (3-MPA), an inhibitor of gluconeogenic

160   phosphoenolpyruvate carboxykinase 1 (*pck1*), to suppress endogenous glucose synthesis (Jurczyk et al,

161   2011). This leads to severe and equal suppression of the maturation of β-cells in the mantle and the core of

162   the islet during the whole hatching period (Figure 3 and Supplemental Movie 5). To probe the optimal

163   endogenous glucose concentration required for β-cell maturation at the early and the late hatching periods,

164   we incubated fish embryos with a combination of 3-MPA and different concentrations of exogenous

165   glucose (3 mM, 5 mM, 8 mM or 20 mM). From 44 to 53 hpf, 3 mM glucose completely rescued the β-cell

166   maturation defects caused by 3-MPA treatment, whereas 8 mM glucose only partially rescued the number

167   of glucose-responsive β-cells in the islet mantle (Figure 3A and C). In contrast, from 60 to 69 hpf, we had

168   to increase the exogenous glucose to 8 mM to fully rescue the phenotype (Figure 3A-D), and 3 mM glucose

169   was insufficient to maintain a normal functional β-cell mass in the islet core (Figure 3A-D). During the

170   entire hatching period, 20 mM glucose performed worst in the rescue experiments, indicative of

171   glucotoxicity at this concentration, as reported in mammalian β-cells previously (Poitout et al, 2006).

172   Therefore, different from vascularization, glucose is required for both β-cells in the islet core and those in

173   the mantle for maturation initiation, function boosting and maintenance. On the other hand, our results also

174   demonstrate that islet vascularization significantly increases the amount of glucose delivered to islet β-cells,

175   initiating the β-cell maturation in the core and boosting all the glucose-responsive β-cells to be more

176   functional.

177

178   ***Calcineurin/NFAT activated by glucose drives β cells maturation***

179   Next, we tried to identify the master signalling pathway triggered by glucose. Recently, activation of

180   calcineurin/NFAT by a glucokinase activator was proposed to mediate β-cells development and function in

181   mice (Goodyer et al, 2012a; Heit et al, 2006). To test whether calcineurin/NFAT act as the primary

182   maturation signalling pathway downstream of glucose, we examined the β-cell maturity after incubating

183   the embryos with calcineurin/NFAT inhibitors and activators. From 36 to 48 hpf, either inhibition of

184   calcineurin with FK506 (Goodyer et al, 2012a; Heit, 2007) or suppression of gluconeogenesis with 3-MPA

185   prevented the appearance of the first glucose-responsive β-cell without affecting β-cell proliferation (Figure

186   4A). In contrast, inhibition of the mTORC pathway with rapamycin abolished β-cell proliferation without

187   affecting its maturation (Figure 4A and B and Supplemental Movie 6). These results suggest that glucose

188   activated calcineurin/NFAT is essential for β-cell maturation initiation.

189   Inhibiting calcineurin or NFAT (with VIVIT (Demozay et al, 2011)) during the hatching period also

190   significantly reduced the number of glucose-responsive β-cells and their maximal Ca^{2+} response amplitude

191   (Figure 4B and Figure 4-Figure Supplement 1). Interestingly, the β-cells that had been already responsive

192 to glucose before the inhibitor treatment were reverted to less matured states (Figure 2-Figure Supplement

193 2), suggesting that calcineurin/NFAT continuous activation is required for the maintenance of the

194 maturation state. On the other hand, direct activation of calcineurin with chlorogenic acid (CGA) (Tong et

195 al, 2007) or NFAT with ProINDY (Ogawa et al, 2010) readily rescued the defective functional maturation

196 of β-cells caused by 3-MPA (Figure 4B, Figure 4-Figure Supplement 1 and Supplemental Movie 6). These

197 results suggest a necessary and sufficient role of calcineurin/NFAT in mediating the effect of glucose in

198 initiating, boosting and sustaining β-cell maturation.

199 To provide further evidence for such a hypothesis, we created and applied a dominant-negative

200 *zebrafish calcineurin A* (*dn-zCnA*). As *CnA* is highly conserved with 81% identity in amino acids between

201 zebrafish and human, we constructed *dn-zCnA* based on the strategy of generating dominant-negative

202 *human calcineurin A* (*dn-hCnA*) (Faure et al, 2007). In Tg(*ins:Rcamp1.07*) genetic background, we

203 generated transient transgenic zebrafish embryos Tg(*ins:EGFP-GSG-T2A-dn-zCnA*), in which the *dn-*

204 *zCnA* is co-expressed with EGFP with a *GSG-T2A* linker under the drive of the insulin promoter. Under

205 TPM, we observed 75.8% ±2.5 Rcamp1.07 positive cells co-express EGFP, indicating 70%-80% β-cells

206 express *dn-zCnA* in Tg(*ins:Rcamp1.07*); Tg(*ins:EGFP-GSG-T2A-dnCnA*) double transgenic fish (Figure

207 4C). When stimulating with 20 mM glucose, we observed a decreased number of glucose-responsive β-

208 cells and smaller maximum Ca^{2+} transients in the responding β-cells in the 72 hpf embryos expressing *dn-*

209 *zCnA* compared with the age-matched controls (Figure 4D and E). The first glucose-responsive β-cells

210 still appeared at the 48 hpf embryos expressing *dn-zCnA*, but all these glucose-responsive β-cells were

211 EGFP negative, indicative of not expressing *dn-zCnA* in these β-cells. Taken together, these results are

212 consistent with the results of pharmacological treatments with calcineurin/NFAT inhibitors, providing

213 convincing evidence that calcineurin/NFAT drives β-cell maturation.

214 Finally, inhibiting calcineurin or suppressing gluconeogenesis severely reduced the number of MafA-

215 positive β-cells at 72 hpf to a similar extent. Direct activating calcineurin, on the other hand, fully rescued

216 the number of MafA-positive β-cells in 3-MPA treated fish (Figure 4F and G). Thus, glucose activates the

217 calcineurin/NFAT signalling pathway to initiate, boost, and sustain the whole process of β-cell maturation,

218 possibly via upregulation of MafA.

219

220 ***Direct activating calcineurin promotes neonatal β-cells towards optimal maturity in isolated mouse islets***

221 ***in vitro***

222 The failure for the core β-cells to mature in the *cloche* mutants and 2,3-BDM-treated embryos could be due

223 to reduced glucose delivery to the islet centre. Indeed, in isolated mouse islets that had no microcirculation,

224 we found a gradually reduced glucose transported into β-cells of the inner layers (Figure 5A-C). To explore

225 whether the requirement of optimal glucose for β-cell maturation could be bypassed *in vitro*, we tried to

226 activate calcineurin/NFAT to promote β-cell maturation in isolated neonatal mouse islets. As we have

227 known, the β-cells of neonatal mouse islets respond poorly to glucose and need more than one week to

228 mature *in vivo* (Blum et al, 2012b). We cultured the neonatal islets from postnatal day 0 (P0) mice for 3

229 days in media supplemented with different concentrations of glucose, in the absence or presence of the

230 calcineurin activator CGA, and evaluated their maturity according to the glucose stimulation index (GSI).

231 Among the different glucose concentrations tested, 11 mM glucose in the culture media was the best in

232 transforming neonatal β-cells in islets to be more glucose-responsive (GSI = 13.0 ± 1.3, Figure 5D and E).

233 Supporting a conserved role of calcineurin in mouse β-cell maturation, combining CGA in the culture media

234 greatly enhanced the GSIs of islets cultured at a glucose concentration ranging from 5.6 mM to 11 mM.

235 Neonatal islets cultured at 11 mM glucose and 56.48 μM CGA exhibited a GSI of 26.5 ± 4.8 (n = 12),

236 similar to that of adult mouse islets cultured at 11 mM glucose (27.3 ± 3.4, n = 4, p = 0.79) (Figure 5D and

237 E). On the other hand, calcineurin inhibitor FK506 notably reduced the GSI of the neonatal islets cultured

238 at 11 mM glucose (Figure 5D and E). As compared to more than one week needed for P0 β-cells to mature

239 *in vivo* (Blum et al, 2012b), our results indicate a greatly accelerated maturation process *in vitro* by using

240 small molecule activators of calcineurin/NFAT, which may also be used to push stem-cell derived immature

241 β-cells towards optimal maturity *in vitro*.

242

243 **Discussion**

244 Here, by taking advantage of the advanced microscopy 2P3A-DSLM technique, we were able to resolve

245 individual β-cells and monitor their functions in an intact living organism. Spatiotemporally, we

246 characterized the maturation of β-cells *in vivo* as two waves that are differentially affected by islet

247 microcirculation: before islet vascularization, locally synthesized glucose initiates the early β-cell

248 maturation from the islet mantle only; islet vascularization significantly increases the amount of glucose

249 delivered to islet β-cells, initiating maturation of β-cells in the islet core and pushing all glucose-responsive

250 β-cells towards further maturity (Figure 6).

251 With classical methods such as immunofluorescence microscopy to observe the expression of

252 maturation markers in fixed samples or ELISA to measure the GSI, β-cells maturation is usually evaluated

253 as a whole. Whether all β-cells in the islets mature at a synchronized pace remains mysterious. By

254 longitudinal imaging β-cell function *in vivo*, we have discovered the apparent heterogeneity of the

255 maturation process inside the islets. In addition, our data also suggests that the dosage effect of glucose on

256 maturation initiation is different from that on function boosting. Suppression of the *in vivo* glucose

257 production with 3-MPA at the early hatching period did not prevent all the mantle β-cells from entering

258 maturation initiation, but limited their glucose-evoked Ca^{2+} responses to the lowest level as those in the

259 core β-cells (Figure 4B). Therefore, the glucose concentrations needed for the conversion of glucose-non-

260 responsive β-cells to glucose-responsive β-cells may be lower than those required for further boosting β-

261 cell function thereafter. Consistently, the glucose concentration needed for the further maturation of β-cells

262 from 55 hpf to 72 hpf increases significantly (Figure 3), reinforcing the concept of a delicately regulated

263 glucose concentration for different steps of β-cell maturation. As zebrafish and mammals share many

264 similarities during pancreatic islet development (Supplemental Table 1), an increasing dosage requirement

265 of glucose for β-cells maturation *in vivo* is very likely to be a conserved mechanism. Consistent with this

266 hypothesis, the plasma glucose level in fetal rodents is relatively low, but starts to increase just before birth

267 and progressively reaches a plateau (above 4 mM) after P2 (Rozzo et al, 2009). From P6 to P20, the plasma

268 glucose further gradually increases from 6 mM to 12 mM (Aguayo-Mazzucato et al, 2006). This period is

269 just accompanied with islet vascularization establishment and glucose-responsive β-cells appear and further

270   maturation (Hole et al, 1988; Reinert et al, 2014; Rozzo et al, 2009). Therefore, β-cell maturation in rodents

271   may also require a dynamically increased glucose concentration, coordinated by islet vascularization.

272   Multiple signalling pathways are known to be activated by glucose to regulate gene transcriptions.

273   These "master switches" include calcineurin/NFAT (Lawrence et al, 2002), the AMP-activated protein

274   kinase, carbohydrate response element-binding protein (Iizuka & Horikawa, 2008; Vaulont et al, 2000),

275   and the hexosamine biosynthetic pathway (Vanderford et al, 2007). Although implication of

276   calcineurin/NFAT in β-cell maturation has been proposed in mice (Goodyer et al, 2012a; Heit et al, 2006),

277   their critical role on the β-cell proliferation mask their effect on the β-cell maturation. For instance, β-cell

278   specific *calcineurin b1* knock-out mice (*RIP-Cre; Cnb1^{Δf}*) did not exhibit any phenotypes until 8-week

279   after birth when β-cell mass starts to reduce (Heit et al, 2006). In contrast, pancreatic endocrine progenitor

280   cell specific *calcineurin b1* knock-out mice (*Ngn3-Cre; Cnb1^{Δlox}*) developed glucose intolerance and

281   diabetes at P20, accompanied with a more than 80% reduction in β-cell mass at P26 (Goodyer et al, 2012a).

282   These data strongly support a critical role of calcineurin/NFAT in β-cell precursor's differentiation and β-

283   cell proliferation, but obscure its role in β-cell maturation. The failure to establish a solid link between

284   calcineurin/NFAT and β-cell maturation may explain why manipulation of this pathway has never been

285   tried to enhance stem cell-derived β-like cells maturation *in vitro*. By imaging β-cell function acquisition

286   and enhancement in zebrafish *in vivo*, we demonstrate that calcineurin/NFAT, downstream of increasing

287   glucose concentrations delivered by the blood circulation, is essential for the initiation, boosting and

288   maintenance of β-cell maturation. The mechanism is inter-species conserved, as activating

289   calcineurin/NFAT could also bypass the deficit of microcirculation in isolated mouse islets, accelerate the

290   *ex vivo* maturation of neonatal mouse β-cells (Figure 5D and E). Currently, different research groups use

291   a variety of glucose concentrations, ranged from 2.8 mM to 20 mM, in the last stage to push β-like cells

292   derived from stem cells *in vitro* to be more functional competent, as nobody knows the ideal condition for

293   the β-cell maturation (Bruin et al, 2015). Obviously, blood vessels are absent from these β-like cell clusters,

294   either. Based on our data, we argue that the lack of spatiotemporal precise glucose delivery to all β-like

295   cells may contribute significantly to their limited glucose responsiveness. On this regard, direct activation

296   of calcineurin/NFAT with small molecules may confer a previously unexplored strategy to push these β-

297   like cell clusters toward maximal maturity *in vitro*.

298   Future imaging of panoramic β-cell mass and function *in vivo* in zebrafish with our system may

299   unravel mechanisms of other important but obscure processes in islet biology, such as regeneration, cell

300   identity or functional changes during disease progression. Understanding these principals may shed light

301   on the ultimate cell replacement therapy to treat diabetes.

302 **Materials and Methods**

303 *Transgenic zebrafish generation*

304 The Tg(*ins:Rcamp1.07*) reporter zebrafish line was generated using meganuclease-mediated transgenesis

305 as previously described (Soroldoni et al, 2009). Briefly, zebrafish BAC_CH211_69I14 (BACPAC

306 Resources Center), which contains the zebrafish *insulin* gene, was modified using Red/ET recombineering

307 technology to replace the coding sequence of insulin with *Rcamp1.07* (Fu et al, 2010). Rcamp1.07-tagged

308 BAC underwent a second round of recombineering for the subcloning of the modified chromosomal locus

309 into a plasmid backbone containing two I-SceI meganuclease sites. The following primers were used for

310 BAC modification:

311   Forward primer: 5' ATGTTTTTGATTGACAGAGATTGTATGTGTGTGTTTGTGTCAGTGTGA

312 CCCGCCACCATGGGTTCTCATC.

313   Reverse primer: 5' CCTGTGTGCAAACAGGTGTTTCTGGCATCGGCGGTGGTCAAATCTCTTC

314 AGGCAGATCGTCAGTCAG.

315   And for subcloning:

316   Forward primer: 5' AGTCCATTAAATAATATCTTGTAGAATTATGTTTTTAAAAAGTACCAAT

317 GCCGTAGGGATAACAGGGTAATTTAAGC.

318   Reverse primer: 5' CAACTTTTTCACAAACACTGACCAAAACAAGCTACATGTTTTAGAGGC

319 ATTAGGGATAACAGGGTAATTGCACTG.

320   The resulting constructs were co-injected with I-SceI meganuclease (Roche) at a DNA concentration of

321 100 ng/µl into one-cell stage zebrafish embryos. These F0 embryos were screened for the transient

322 expression of Rcamp1.07 in the pancreatic islet at 48 hpf using a fluorescence stereomicroscope. The

323 positive F0 founders were raised to adults and were screened by visual inspection of their F1 progenies

324 from outcrossing with the wild-type AB strain. Based on the intensity of the fluorescence signal, one

325 founder was selected, and subsequent generations were propagated and expanded.

326   The Tg(*ins:EGFP-GSG-T2A-dn-zCnA*) zebrafish line was generated using Tol2 transposase RNA-

327 mediated transgenesis as previously described. Briefly, *dn-zCnA* was constructed by deleting the auto-

328 inhibitory and the calmodulin-binding domains through introducing a stop codon at the N396 amino acid

329 and by mutating the histidine at the position 152, a phosphatase-active site, to glutamine. The GSG-T2A

330 peptide was used to separating EGFP and dn-zCnA elements. The EGFP-GSG-T2A-dn-zCnA fragment

331 was cloned downstream of 2.1 kb of the proximal insulin promoter and into a Tol2 plasmid by ClonExpress

332 system. The final construct was injected along with Tol2 transposase RNA into Tg(*ins:Rcamp1.07*) eggs to

333 generate mosaic Tg(*ins:EGFP-GSG-T2A-dn-zCnA*); Tg(*ins:Rcamp1.07*) F0 fish for imaging analysis.

334

335 ***Zebrafish care and handling***

336 The wild-type AB strain and transgenic fish were maintained and handled according to the institutional

337 guidelines of animal usage and maintenance of Peking University. *Tg(ins:EGFP)* fish were from Dr. Lin

338 Shuo at UCLA; *Tg(flk1:mCherry)* fish were from Dr. Zhang Bo at PKU; *Tg(flk1:GFP)* fish were from Dr.

339 Chen Jau-Nian at UCLA. *Tg(ins:Rcamp1.07)* was crossed with heterozygous *cloche*[m39] to obtain

340 *Tg(ins:Rcamp1.07);cloche*[m39]*/+* zebrafish. *Tg(ins:Rcamp1.07);cloche*[m39]*/ cloche*[m39] embryos from the

341 crossing of *Tg(ins:Rcamp1.07);cloche*[m39]*/+* with *cloche*[m39]*/+* fish were used for the imaging experiments.

342 For imaging, 0.002% phenylthiourea (PTU, Sigma) was added at 12 hpf to prevent pigment synthesis. Prior

343 to live imaging, embryos were anaesthetized with 0.01% tricaine (Sigma).

344 Pharmacological treatment. Heterozygous *Tg(ins:Rcamp1.07)* embryos were used for

345 pharmacological treatment and imaging analysis. All chemicals were prepared as high-concentration stocks

346 and were diluted in E3 medium to final concentrations for treatment, which were carefully selected to be

347 non-toxic and effective. To test the pharmacological effect of the chemicals on the functional maturation

348 of pancreatic β cells, the embryos were treated with each chemical for 9 hours, either from 44 to 53 hpf or

349 from 60 to 69 hpf; the embryos then recovered for 3 h after E3 medium was used to completely wash out

350 the chemical, and imaging analysis was carried out at 56 hpf or at 72 hpf, respectively. For the

351 pharmacological treatment of zebrafish embryos, 10 mM 2,3-butanedione monoxime (2,3-BDM, Sigma)

352 was used to block blood circulation; 3 mM 3-mercaptopicolinic acid (3-MPA, Santa Cruz) was used to

353 inhibit endogenous glucose production; 141.2 μM chlorogenic acid (CGA, Sigma) or 10 μM FK506

354 (Invivogen) was used to activate or inhibit calcineurin, respectively; and 2.5 μM ProINDY (Tocris) or 20

355 μM VIVIT peptide (Tocris) was used to activate or inhibit NFAT, respectively.

356

Wide field and 2P3A-DSLM imaging

358 For the wide field time-lapse imaging, the images were captured using an Olympus inverted fluorescence

359 microscope with a $10\times/0.4$ objective. D-Glucose stock solution was added to the E3 medium for a final

360 concentration of 20 mM during stimulation. The images were collected with MetaMorph software and

361 analysed with Fiji software.

362 High-resolution images of pancreatic β-cells and blood vessels in live zebrafish embryos were captured

363 with 2P3A-DSLM equipped with two $40\times/0.8$ water lenses as previously described (Zong et al, 2015).

364 Briefly, the anaesthetized embryos were embedded in a 1% ultra-pure agarose (Invitrogen) cylinder and

365 then immersed in a homemade chamber with E3 medium containing 0.01% tricaine. D-glucose stock was

366 added to the E3 medium to reach a final concentration of 20 mM to stimulate the fish embryos. For the 2D

367 time-lapse imaging experiments that were used for statistical analysis, the islet was optically sectioned into

368 5-6 layers to ensure that the calcium transients of all β-cells within the islet were recorded. For fast

369 volumetric imaging and reconstruction of calcium transients within the whole islet, the islet was optically

370 sectioned into 25 layers. Each layer was captured 5 times with an 8-ms exposure time and was averaged as

371 one single image. Images were collected by the HCImage software (Hamamatsu) and processed with R-L

372 deconvolution by Fiji software. The volumetric calcium transients were reconstructed with Amira software

373 (FEI).

374

Comparison among 1P-SPIM, TPM and 2P3A-DSLM in 3D imaging of islet in vivo

376 For 1P-SPIM imaging, we used a homemade SPIM setup equipped with a $40\times/0.8$ water lens. For TPM

377 imaging, we used a fast resonant-scanned TPM equipped with a $40\times/0.8$ water lens. The same 72 hpf

378 zebrafish samples were sequentially imaged with 1P-SPIM, TPM and 2P3A-DSLM. Under each

379 configuration, the whole islet was optically sectioned by 100 planes (z-step: 500 nm) with an exposure time

380 of 150 ms per frame. Images were collected by HCImage software and processed with R-L deconvolution

381 by Fiji software.

382

Whole-mount immunofluorescence and confocal imaging

The embryos were fixed in 4% paraformaldehyde (PFA, AppliChem) at 4 ℃ overnight. After the PFA was washed away, the embryos were dehydrated using a series of methanol (25%, 50%, 75% and 100%) and stored at -20 ℃. When necessary, the embryos were rehydrated using a series of methanol (100%, 75%, 50% and 25%), permeabilized in Proteinase K (10 μg/ml, TransGen), washed in PBST (PBS + 0.1% Tween-20) and then fixed again in 4% PFA at room temperature (RT). After being blocked with PBST containing 0.2% bovine serum albumin (BSA, AppliChem) and 5% fetal bovine serum (Gibco) for 1 h at RT, the embryos were incubated with primary antibodies overnight at 4 ℃. Then, secondary antibodies were applied at 4 ℃ overnight after thorough washing. The primary antibodies included monoclonal rat anti-mCherry antibody (1:200, Thermo, used to detect Rcamp1.07), polyclonal guinea pig anti-insulin antibody (1:200, Dako) and polyclonal rabbit anti-MafA antibody (1: 50, Sigma). The secondary antibodies were Alexa Fluor 568 goat anti-rat IgG (1: 500, Thermo), DyLight 488 goat anti-guinea pig IgG (1: 500, Thermo), DyLight 550 goat anti-guinea pig IgG (1: 500, Thermo) and DyLight 488 goat anti-rabbit IgG (1: 500, Thermo). Before imaging, the samples were dehydrated in 100% methanol and mounted in mounting solution containing one volume of benzyl alcohol (Sigma) and two volumes of benzyl benzoate (Sigma) with their right side facing the coverslips. The images were collected by MetaMorph software using an Olympus spinning-disc confocal microscope and processed by Fiji software.

Embedding and cryostat sectioning

The embryos were fixed in 4% PFA at 4 ℃ overnight. After being washed, the embryos were dehydrated in 30% sucrose (Sigma) and then transferred to embedding chambers filled with OCT compound (Tissue Tek®). After embedding, the samples were frozen in liquid nitrogen as soon as possible. Sectioning was performed using a Leica CM1900 Cryostat set to 10 μm thickness and a −25 °C chamber temperature. The sections were collected and kept at -20 ℃ in a sealed slide box. Immunofluorescence staining was performed as described above. For nuclear staining, the samples were incubated with 2 μg/ml DAPI (Solarbio) for 10 minutes. After an extensive wash, the samples were mounted in 80% glycerol (Sigma) and imaged using an Olympus spinning-disc confocal microscope.

410

Uptake of the fluorescent D-glucose analogue by β-cells in mouse islets

412 For this study, 8-week-old mouse islets were isolated and cultured in RPMI 1640 medium containing 7 mM

413 glucose for 2 days (Wang et al, 2016). Before imaging, the islets were washed twice with Krebs (KRB)

414 buffer (129 mM NaCl, 4.7 mM KCl, 1 mM $CaCl_2 \cdot 2H_2O$, 1.2 mM $MgSO_4$, 1.2 mM KH_2PO_4, 5 mM

415 $NaHCO_3$, 10 mM HEPES, 0.5% BSA) and then pre-incubated in 7 mM 2-(N-(7-nitrobenz-2-oxa-1,3-diazol-

416 4-yl)Amino)-2-deoxyglucose (2-NBDG) dissolved in KRB buffer for 10 min at 37℃. After thoroughly

417 washing, z-stack images of the islets were captured with a TPM (Zeiss 710). The 2-NBDG signal was

418 excited at 920 nm and collected between 510 nm and 540 nm.

419

In vitro culture of mouse islets and measurement of glucose-stimulated insulin secretion

421 Adult islets from 8-week-old mice were isolated as previously described (Wang et al, 2016). For P0 mouse

422 islet isolation, pancreata were dissected directly without perfusion and digested with 0.5 mg/ml Collagenase

423 P (Roche). The isolated islets were cultured for 3 days in RPMI1640 media containing different

424 concentrations of glucose (0.5 mM, 2.8 mM, 5.6 mM, 7 mM, 11 mM, 15 mM and 20 mM) combined or not

425 combined with CGA (56.48 μM). The culture medium was changed every day. 10 islets with similar sizes

426 were selected and pre-incubated in KRB buffer for 3 hours at 37℃ in a 5% CO_2 incubator. The islets were

427 then transferred into low glucose (3 mM) KRB buffer and incubated for 1 hour at 37℃, 5% CO_2. The

428 supernatant was collected for measuring basal insulin secretion. The same islets were further transferred

429 into high glucose (20 mM) KRB buffer for 1 hour incubation at 37℃, 5% CO_2. The supernatant was

430 collected, stored at -20℃ and later the insulin content was measured with the Rat/Mouse insulin ELISA kit

431 (Millipore).

432

Statistical analysis

434 All data were analysed using GraphPad Prism 6 software. Average results were displayed as the mean

435 values ± SEM. Statistical significance was evaluated using either Student's t-test for single Gaussian-

436   distributed datasets or Mann-Whitney rank sum test for non-single Gaussian-distributed datasets. The

437   asterisks * and ** denote statistical significance with *p* values less than 0.05 or 0.01, respectively.

438

439   ***Study approval***

440   Generation of the transgenic zebrafish lines, *in vivo* imaging of the living zebrafish embryos, and all the

441   other experiments about zebrafish and mouse islets were approved by the IACUC of Peking University.

442

443

444

445

446

447

448

449

450

451

452

453

454

455

456

457

Acknowledgments

Author contributions

Y. L. conceived the project. L.C. and Y.L. directed the study. J.Z., L.C. and Y.L. designed the research. J.Z., W.Z., Y.W., J.S., D.G., Y.Z., R.W., F.N., X.W., X.Z., A.W., Y.Z., and Y.L. performed the experiments. J.X. provided critical fish lines and fish facility. J.Z., L.C. and Y.L. analyzed the data and wrote the manuscript.

Competing interests

The authors declare that they have no conflict of interest.

References

Aguayo-Mazzucato C, Sanchez-Soto C, Godinez-Puig V, Gutierrez-Ospina G, Hiriart M (2006) Restructuring of Pancreatic Islets and Insulin Secretion in a Postnatal Critical Window. *Plos One* **1**

Avolio F, Pfeifer A, Courtney M, Gjerne E, Ben-Othman N, Vieira A, Druelle N, Faurite B, Collombat P (2013) From Pancreas Morphogenesis to beta-Cell Regeneration. *Curr Top Dev Biol* **106:** 217-238

Bartman T, Walsh EC, Wen KK, McKane M, Ren J, Alexander J, Rubenstein PA, Stainier DY (2004) Early myocardial function affects endocardial cushion development in zebrafish. *PLoS Biol* **2:** E129

Blum B, Hrvatin S, Schuetz C, Bonal C, Rezania A, Melton DA (2012a) Functional beta-cell maturation is marked by an increased glucose threshold and by expression of urocortin 3. *Nat Biotechnol* **30:** 261-264

Blum B, Hrvatin SS, Schuetz C, Bonal C, Rezania A, Melton DA (2012b) Functional beta-cell maturation is marked by an increased glucose threshold and by expression of urocortin 3. *Nat Biotechnol* **30:** 261-264

Borden P, Houtz J, Leach SD, Kuruvilla R (2013) Sympathetic innervation during development is necessary for pancreatic islet architecture and functional maturation. *Cell Rep* **4:** 287-301

Bruin JE, Rezania A, Kieffer TJ (2015) Replacing and safeguarding pancreatic beta cells for diabetes. *Sci Transl Med* **7:** 316ps323

Carvalho CP, Barbosa HC, Britan A, Santos-Silva JC, Boschero AC, Meda P, Collares-Buzato CB (2010) Beta cell coupling and connexin expression change during the functional maturation of rat pancreatic islets. *Diabetologia* **53:** 1428-1437

Cleaver O, Dor Y (2012) Vascular instruction of pancreas development. *Development* **139:** 2833-2843

Demozay D, Tsunekawa S, Briaud I, Shah R, Rhodes CJ (2011) Specific glucose-induced control of insulin receptor substrate-2 expression is mediated via Ca2+-dependent calcineurin/NFAT signaling in primary pancreatic islet beta-cells. *Diabetes* **60:** 2892-2902

Faure C, Corvol JC, Toutant M, Valjent E, Hvalby O, Jensen V, El Messari S, Corsi JM, Kadare G, Girault JA (2007) Calcineurin is essential for depolarization-induced nuclear translocation and tyrosine phosphorylation of PYK2 in neurons. *J Cell Sci* **120:** 3034-3044

Field HA, Dong PD, Beis D, Stainier DY (2003a) Formation of the digestive system in zebrafish. II. Pancreas morphogenesis. *Dev Biol* **261:** 197-208

524   Field HA, Dong PDS, Beis D, Stainier DYR (2003b) Formation of the digestive system in zebrafish. II. Pancreas
525   morphogenesis. *Dev Biol* **261:** 197-208

526

527   Fu J, Teucher M, Anastassiadis K, Skarnes W, Stewart AF (2010) A recombineering pipeline to make conditional
528   targeting constructs. *Methods Enzymol* **477:** 125-144

529

530   Goodyer WR, Gu X, Liu Y, Bottino R, Crabtree GR, Kim SK (2012a) Neonatal beta cell development in mice and
531   humans is regulated by calcineurin/NFAT. *Dev Cell* **23:** 21-34

532

533   Goodyer WR, Gu XY, Liu YH, Bottino R, Crabtree GR, Kim SK (2012b) Neonatal beta Cell Development in Mice
534   and Humans Is Regulated by Calcineurin/NFAT. *Dev Cell* **23:** 21-34

535

536   Guillemain G, Filhoulaud G, Da Silva-Xavier G, Rutter GA, Scharfmann R (2007) Glucose is necessary for embryonic
537   pancreatic endocrine cell differentiation. *J Biol Chem* **282:** 15228-15237

538

539   Heit JJ (2007) Calcineurin/NFAT signaling in the beta-cell: From diabetes to new therapeutics. *Bioessays* **29:** 1011-
540   1021

541

542   Heit JJ, Apelqvist AA, Gu X, Winslow MM, Neilson JR, Crabtree GR, Kim SK (2006) Calcineurin/NFAT signalling
543   regulates pancreatic beta-cell growth and function. *Nature* **443:** 345-349

544

545   Hole RL, Piansmith MCM, Sharp GWG (1988) Development of the Biphasic Response to Glucose in Fetal and
546   Neonatal Rat Pancreas. *Am J Physiol* **254:** E167-E174

547

548   Huang H, Vogel SS, Liu N, Melton DA, Lin S (2001) Analysis of pancreatic development in living transgenic
549   zebrafish embryos. *Mol Cell Endocrinol* **177:** 117-124

550

551   Iizuka K, Horikawa Y (2008) ChREBP: A glucose-activated transcription factor involved in the development of
552   metabolic syndrome. *Endocr J* **55:** 617-624

553

554   Jurczyk A, Roy N, Bajwa R, Gut P, Lipson K, Yang C, Covassin L, Racki WJ, Rossini AA, Phillips N, Stainier DY,
555   Greiner DL, Brehm MA, Bortell R, diIorio P (2011) Dynamic glucoregulation and mammalian-like responses to
556   metabolic and developmental disruption in zebrafish. *Gen Comp Endocrinol* **170:** 334-345

557

558   Kushner JA, MacDonald PE, Atkinson MA (2014) Stem Cells to Insulin Secreting Cells: Two Steps Forward and
559   Now a Time to Pause? *Cell Stem Cell* **15:** 535-536

560

561   Lawrence MC, Bhatt HS, Easom RA (2002) NFAT regulates insulin gene promoter activity in response to synergistic
562   pathways induced by glucose and glucagon-like peptide-1. *Diabetes* **51:** 691-698

563

564 Nair G, Hebrok M (2015) Islet formation in mice and men: lessons for the generation of functional insulin-producing

565 beta-cells from human pluripotent stem cells. *Curr Opin Genet Dev* **32:** 171-180

566

567 Ogawa Y, Nonaka Y, Goto T, Ohnishi E, Hiramatsu T, Kii I, Yoshida M, Ikura T, Onogi H, Shibuya H, Hosoya T,

568 Ito N, Hagiwara M (2010) Development of a novel selective inhibitor of the Down syndrome-related kinase Dyrk1A.

569 *Nat Commun* **1:** 86

570

571 Ohkura M, Sasaki T, Kobayashi C, Ikegaya Y, Nakai J (2012) An improved genetically encoded red fluorescent Ca2+

572 indicator for detecting optically evoked action potentials. *Plos One* **7:** e39933

573

574 Omar B, Ahlkvist L, Yamada Y, Seino Y, Ahren B (2016) Incretin hormone receptors are required for normal beta

575 cell development and function in female mice. *Peptides* **79:** 58-65

576

577 Pagliuca FW, Millman JR, Gurtler M, Segel M, Van Dervort A, Ryu JH, Peterson QP, Greiner D, Melton DA (2014)

578 Generation of Functional Human Pancreatic beta Cells In Vitro. *Cell* **159:** 428-439

579

580 Pan FC, Wright C (2011) Pancreas organogenesis: from bud to plexus to gland. *Dev Dyn* **240:** 530-565

581

582 Poitout V, Hagman D, Stein R, Artner I, Robertson RP, Harmon JS (2006) Regulation of the insulin gene by glucose

583 and fatty acids. *J Nutr* **136:** 873-876

584

585 Reinert RB, Cai Q, Hong JY, Plank JL, Aamodt K, Prasad N, Aramandla R, Dai CH, Levy SE, Pozzi A, Labosky PA,

586 Wright CVE, Brissova M, Powers AC (2014) Vascular endothelial growth factor coordinates islet innervation via

587 vascular scaffolding. *Development* **141:** 1480-1491

588

589 Rezania A, Bruin JE, Arora P, Rubin A, Batushansky I, Asadi A, O'Dwyer S, Quiskamp N, Mojibian M, Albrecht T,

590 Yang YH, Johnson JD, Kieffer TJ (2014) Reversal of diabetes with insulin-producing cells derived in vitro from

591 human pluripotent stem cells. *Nat Biotechnol* **32:** 1121-1133

592

593 Rozzo A, Meneghel-Rozzo T, Delakorda SL, Yang SB, Rupnik M (2009) Exocytosis of Insulin In Vivo Maturation

594 of Mouse Endocrine Pancreas. *Ann Ny Acad Sci* **1152:** 53-62

595

596 Shah SR, Esni F, Jakub A, Paredes J, Lath N, Malek M, Potoka DA, Prasadan K, Mastroberardino PG, Shiota C, Guo

597 P, Miller KA, Hackam DJ, Burns RC, Tulachan SS, Gittes GK (2011) Embryonic mouse blood flow and oxygen

598 correlate with early pancreatic differentiation. *Dev Biol* **349:** 342-349

599

600 Shih HP, Wang A, Sander M (2013) Pancreas Organogenesis: From Lineage Determination to Morphogenesis. *Annu*

601 *Rev Cell Dev Bi* **29:** 81-105

602

603 Soroldoni D, Hogan BM, Oates AC (2009) Simple and efficient transgenesis with meganuclease constructs in

604 zebrafish. *Methods Mol Biol* **546:** 117-130

605

606   Tehrani Z, Lin S (2011) Endocrine pancreas development in zebrafish. *Cell Cycle* **10:** 3466-3472

607

608   Tiso N, Moro E, Argenton F (2009) Zebrafish pancreas development. *Mol Cell Endocrinol* **312:** 24-30

609

610   Tong L, Song Y, Jia Z, Zhang W, Wei Q (2007) Calmodulin-dependent activation of calcineurin by chlorogenic acid.
611   *IUBMB Life* **59:** 402-407

612

613   Tsuji N, Ninov N, Delaware M, Osman S, Roh AS, Gut P, Stainier DYR (2014) Whole Organism High Content
614   Screening Identifies Stimulators of Pancreatic Beta-Cell Proliferation. *Plos One* **9**

615

616   Vanderford NL, Andrali SS, Ozcan S (2007) Glucose induces MafA expression in pancreatic beta cell lines via the
617   hexosamine biosynthetic pathway. *J Biol Chem* **282:** 1577-1584

618

619   Vaulont S, Vasseur-Cognet M, Kahn A (2000) Glucose regulation of gene transcription. *J Biol Chem* **275:** 31555-
620   31558

621

622   Wang L, Liu T, Xu L, Gao Y, Wei Y, Duan C, Chen GQ, Lin S, Patient R, Zhang B, Hong D, Liu F (2013) Fev
623   regulates hematopoietic stem cell development via ERK signaling. *Blood* **122:** 367-375

624

625   Wang Y, Han C, Zhu W, Wu Z, Liu Y, Chen L (2016) An optical method to evaluate both mass and functional
626   competence of pancreatic alpha- and beta-cells. *J Cell Sci* **129:** 2462-2471

627

628   Yamaoka T, Itakura M (1999) Development of pancreatic islets (Review). *Int J Mol Med* **3:** 247-261

629

630   Zhou Q, Law AC, Rajagopal J, Anderson WJ, Gray PA, Melton DA (2007) A multipotent progenitor domain guides
631   pancreatic organogenesis. *Dev Cell* **13:** 103-114

632

633   Zong W, Zhao J, Chen X, Lin Y, Ren H, Zhang Y, Fan M, Zhou Z, Cheng H, Sun Y, Chen L (2015) Large-field high-
634   resolution two-photon digital scanned light-sheet microscopy. *Cell Res* **25:** 254-257

635
636
637

638

639

640

641

642   **Figure Legends**

643

644   **Figure 1. Visualization and characterization of the β-cell maturation process *in vivo* by 2P3A-DSLM.**

645   (*A*) An abbreviated scheme of the dual-colour 2P3A-DSLM imaging system. (*B*) 3D-projection of all

646   pancreatic β-cells in a living 72 hpf *Tg(ins:Rcamp1.07)* zebrafish embryo. The different colours in the

647   colour bar represent different depth of the islet. (*C*) The increasing rates of total β-cell and glucose-

648   responsive β-cell numbers at different stages from 28 to 74 hpf. n = 10-16 embryos for each stage. (*D*)

649   Whole-mount immunofluorescent labelling of insulin and MafA in embryos at 48, 56 and 72 hpf (left).

650   Representative immunofluorescent labelling images of cryostat sections of 72 hpf zebrafish embryos (right).

651   (*E*) Quantifications of MafA-positive β-cells and glucose-responsive β-cells at the indicated stages. n = 4-

652   6 embryos for each condition. **$P<0.01$. (*F*) An illustration of glucose-responsive (red) and glucose non-

653   responsive (green) β-cells of the islets in live *Tg(ins:Rcamp1.07) Tg(ins:EGFP)* embryos at 48, 56 and 72

654   hpf. (*G*) Average traces of glucose-triggered maximum Ca^{2+} transients at the indicated stages. n = 10-16

655   embryos for each condition. (Scale bars: 10 μm; scale bars apply to *D* and *F*.) See also Figure 1-Figure

656   Supplement 1, 2 and 3, and Supplemental Movies 1, 2 and 3.

657

658   **Figure 2. Sequential maturation of β-cells in the mantle and the core of the islet from the early to the**

659   **late hatching period, which is coordinated with islet microcirculation.** (*A*) Representative 3D-

660   projections of β-cells (green) and neighbouring blood vessels (red) at different stages in live

661   *Tg(ins:EGFP);Tg(flk1:mCherry)* embryos. (*B*) The comparison of the increasing rate of β-cells adjacent to

662   the vascular endothelium (VE) with that of glucose-responsive β-cells at different stages from 28 to 74 hpf.

663   n = 4-7 embryos for each stage. (*C*) An illumination of classification of β-cells into two populations, cells

664   in the mantle (green) and in the core (red) of the islet. (*D*) Time-dependent increases in the glucose-

665   responsive β-cells from the mantle (dark) and the core (red) of the islet. n = 10-16 embryos for each stage.

666   (*E-F*) Time-dependent increases in the maximum amplitude (*E*) and the speed (*F*) of the glucose-triggered

667   Ca^{2+} transients in β-cells from the mantle and the core of the islet. n = 10-16 embryos for each stage in *E*

668   and *F*. (*G*) Representative 3D-projections of the β-cells (red) and neighbouring blood vessels (green) in live

669 wild-type or *cloche*^{-/-} *Tg(ins:Rcamp1.07);Tg(flk1:GFP)* embryos. (*H-I*) Numbers of glucose-responsive β-

670 cells (*H*) and their maximal Ca^{2+} responses to glucose (*I*) in the mantle and core of the islets in *cloche*^{-/-}

671 mutants and 2,3-BDM-treated embryos. n = 4-6 embryos for each stage in *H* and *I*. *$P<0.05$, **$P<0.01$.

672 (Scale bars: 10 μm; scale bars apply to *A*, *C* and *G*.) See also Figure 2-Figure Supplement 1 and

673 Supplemental Movie 4.

674

675 **Figure 3. Different concentrations of glucose are required for inducing optimal β-cell maturation at**

676 **different maturation stages.** (*A-B*) Numbers of glucose-responsive β-cells (*A*) and their maximal Ca^{2+}

677 responses to glucose (*B*) in the mantle and in the core of the islets from embryos treated with 3-MPA and

678 different concentrations of glucose. n = 4-8 embryos for each condition in A and B. *$P<0.05$, **$P<0.01$. (*C-*

679 *D*) The recovery ratios of glucose-responsive β-cells (*C*) and their maximal Ca^{2+} responses to glucose (*D*)

680 by different concentrations of exogenous glucose while the endogenous glucose production was inhibited

681 by 3-MPA. The ratios are represented as the normalized numbers of glucose-responsive β-cells or the

682 normalized maximal amplitudes of the calcium transients relative to those of the control embryos. n = 4-8

683 embryos for each condition in *C* and *D*. *$P<0.05$, **$P<0.01$; ns, not significant. See also Figure 3-Figure

684 Supplement 1 and Supplemental Movie 5.

685

686 **Figure 4. Calcineurin/NFAT acts as the master regulator downstream of glucose to initiate and**

687 **sustain β-cell maturation.** (*A*) Numbers of total β-cells (left) and glucose-responsive β-cells (right) in 48

688 hpf embryos that had been treated with the indicated reagents. n = 4-8 embryos for each condition. *$P<0.05$,

689 **$P<0.01$; ns, not significant. (*B*) Numbers of glucose-responsive β-cells (left) and their maximal

690 amplitudes of Ca^{2+} transients in glucose-responsive β-cells (right) in the mantle and core of the islet in 56

691 hpf embryos that had been treated with the indicated reagents. n = 5-9 embryos for each condition. *$P<0.05$,

692 **$P<0.01$; ns, not significant. (*C*) Representative TPM images of Rcamp1.07 (left), EGFP (middle) and the

693 merged images (right) of the same islet cells in 72 hpf living *Tg(ins:Rcamp1.07);Tg(ins:EGFP-GSG-T2A-*

694 *dn-zCnA)* embryos. (*D-E*) Numbers of glucose-responsive β-cells (*D*) and their maximal Ca^{2+} responses to

695 glucose (*E*) in the age-matched control and the embryos expressing *dn-zCnA* at 48 and 72 hpf. n = 3-4

696   embryos for each stage in *D* and *E*. *P<0.05, **P<0.01; ns, not significant. (*F*) Immunofluorescent labelling

697   of insulin and MafA in 72 hpf embryos that had been treated with the indicated reagents. (*G*) Quantifications

698   of MafA-positive β-cells in 72 hpf embryos that had been treated with the indicated reagents. n = 4-6

699   embryos for each condition. **P<0.01; ns, not significant. (Scale bars: 10 μm; scale bars apply to *C* and *F*.)

700   See also Figure 4-Figure Supplement 1 and Supplemental Movie 6.

701

702   **Figure 5. Direct activating calcineurin readily pushes neonatal mouse β-cells in isolated islets towards**

703   **optimal maturation *in vitro*.** (*A*) Significantly reduced glucose uptake in the core of the islets *in vitro*

704   represented as the TPM image of an islet pre-incubated with 7mM 2-NBDG (a fluorescent D-glucose analog)

705   for 10 min. (*B*) Profile plot of fluorescent intensity versus distance indicated in A (white line with arrow).

706   (*C*) Normalized fluorescent intensity of β-cells in each layer of the islet in A. *P<0.05, **P<0.01. (*D*)

707   Glucose-stimulated insulin secretion from neonatal mouse islets stimulated with low and high glucose, after

708   isolation from P0 mice and culturing *in vitro* for 3 days in different media. Insulin secretion of adult islets

709   from 8-week-old mice after 3 days of culturing in media with 11 mM glucose is also shown. n = 4-10

710   experiments for each condition. *P<0.05, **P<0.01; ns, not significant. (*E*) GSIs of the neonatal islets and

711   the adult islets described in *D*. n = 4-10 experiments for each condition. **P<0.01; ns, not significant.

712

713   **Figure 6. An inter-species conserved model of microcirculation-coordinated, glucose-triggered,**

714   **calcineurin/NFAT-dependent β-cell maturation *in vivo*.** At approximately 48 hpf, locally synthesized

715   glucose (~3 mM) initiates glucose responsiveness of β-cells exclusively in the islet mantle. After 60 hpf,

716   islet vascularization enables the efficient delivery of glucose through the blood circulation to the islet core

717   to trigger the internal cells to mature. Both the mantle and the core β-cells sense a more than 2-fold increase

718   in glucose (~8 mM), which pushes them to further maturity. Maturation of all β-cells in the islet depends

719   on the glucose-activated calcineurin/NFAT pathway, the master regulators of MafA expression and β-cell

720   function acquisition.

721

722   **Figure 1-Figure Supplement 1. Specific expression of Rcamp1.07 in pancreatic β-cells in**

723   ***Tg(ins:Rcamp1.07)* zebrafish.** (*A*) An illustration shows the protocol for generating the *Tg(ins:Rcamp1.07)*

724   fish line. (*B*) *Tg(ins:Rcamp1.07)*-positive fish with Rcamp1.07 fluorescent signals in the islet region under

725   a wide field microscope. (*C-E*) Representative dual-colour 2P3A-DSLM images of Rcamp1.07 (*C*), EGFP

726   (*D*) and the merged images (*E*) of the same islet cells in 72 hpf living *Tg(ins:Rcamp1.07);Tg(ins:EGFP)*

727   embryos. (*F*) The co-localization of Rcamp1.07 and EGFP was analysed by Mander's intensity correlation

728   (Fiji plugin), and the Pearson's R value was 0.93. **(*G-J*)** Representative confocal images of

729   immunofluorescently labelled Rcamp1.07 (*G*), insulin (*H*), DAPI labelling (*I*) and the merged images (*J*)

730   of the same islet cells in 72 hpf *Tg(ins:Rcamp1.07)* embryos. (Scale bars: 10 μm; scale bars apply to *C-E*

731   and *G-J*.)

732

733   **Figure 1-Figure Supplement 2. Visualization of glucose-stimulated calcium transients in β-cells in**

734   **living *Tg(ins:Rcamp1.07)* embryos under a wide field microscope.** *Tg(ins:Rcamp1.07)* embryos were

735   embedded in a 1% ultra-pure agarose cylinder and immersed in a 35 mm plastic chamber filled with E3

736   medium containing 0.01% tricaine. Images were captured once every minute with a 150 ms exposure time.

737   At the 10 min time point, 20 mM glucose was added. (*A*) Representative images of Rcamp1.07 in the

738   pancreatic islet of a 72 hpf live *Tg(ins:Rcamp1.07)* embryo after stimulation with 20 mM glucose. Montages

739   started from 3 min after glucose application and are shown at 3-min intervals. Arrows indicate two

740   representative regions within the islet. (*B*) Time courses of calcium transients from the regions marked in

741   *A*. (Scale bar: 50 μm.)

742

743   **Figure 1-Figure Supplement 3. Quantification of glucose-responsive β-cells and evaluation of their**

744   **maturation states.** (*A*) Quantification of glucose-responsive β-cells at different stages from 24 to 72 hpf.

745   *$^{*}P<0.05$. (*B*) An illustration of the two parameters describing the kinetics of glucose-stimulated Ca^{2+}

746   transients: the maximum amplitude (Max ΔF/F) and the speed of the Ca^{2+} response (time to rise); the latter

747   was defined as the delay between the time of glucose application and the time when the increase in

748   cytoplasmic Ca^{2+} reached half of the Max ΔF/F. (*C*) Average speeds (time to rise) of the Ca^{2+} responses in

749   glucose-responsive β cells from 48 to 72 hpf. *$P<0.05$. (*D*) Average maximum amplitudes of Ca^{2+} transients

750   in glucose-responsive β-cells from 48 to 72 hpf. **$P<0.01$.

751

752   **Figure 2-Figure Supplement 1. Islet vascularization does not affect the total β-cell number, but**

753   **correlates with the acquisition of glucose-responsiveness of β-cells.** (*A*) Quantification of glucose-

754   responsive β-cells adjacent or non-adjacent to blood vessels from 44 to 72 hpf. n = 4-7 embryos for each

755   condition. (*B*) Quantification of pancreatic β-cells adjacent or non-adjacent to VE cells from 36 to 72 hpf.

756   n = 8 embryos for each condition. *$P<0.05$, **$P<0.01$. (*C*) Quantification of total β-cells in wild-type or

757   *cloche*^{-/-} embryos at 48, 56, and 72 hpf. n = 3-4 embryos for each condition.

758

759   **Figure 3-Figure Supplement 1. Blocking blood circulation at the late hatching period stops β-cells at**

760   **a functional status equivalent to 60 hpf embryos, whereas inhibiting the glucose/calcineurin/NFAT**

761   **pathway severely reverts glucose-responsive β-cells to less matured states.** (*A*) The experimental design

762   for *B* and *C* in which *Tg(ins:Rcamp1.07)* embryos at 60 hpf were treated with different reagents for 9 h and

763   then washed in the normal E3 medium for 3 h before imaging. (*B-C*) Quantification of glucose-responsive

764   β-cells (*B*) and their maximal ΔF/F (*C*) in 60 hpf controls (n = 4), 72 hpf *cloche*^{-/-} mutants (n = 4) and 72

765   hpf embryos that had been treated with 2,3-BDM (n = 4), 3-MPA (n = 10), FK506 (n = 6) or VIVIT (n =

766   6). *$P<0.05$, **$P<0.01$; ns, not significant.

767

768   **Figure 4-Figure Supplement 1. Glucose activates calcineurin/NFAT to finish the final maturation of**

769   **pancreatic β-cells during the late hatching period.** *Tg(ins:Rcamp1.07)* embryos at 60 hpf were treated

770   with different reagents for 9 h and then washed in the normal E3 medium for 3 h before imaging. (*A-B*)

771   Quantification of glucose-responsive β-cells (*A*) and their maximal ΔF/F in glucose-responsive β-cells (*B*)

772   in the mantle and core of the islet in DMSO-treated controls, rapamycin-treated embryos, 3-MPA-treated

773   embryos, FK506-treated embryos, VIVIT-treated embryos, 3-MPA and CGA co-treated embryos and 3-

774   MPA and ProINDY co-treated embryos at 72 hpf. n = 5-9 embryos for each condition. *$P<0.05$, **$P<0.01$;

775   ns, not significant.

776

Supplemental Table 1. Comparison of the critical events and the time windows in zebrafish and mouse pancreas development.

779

Supplemental Movie 1. Time-lapse images of glucose-stimulated calcium transients in pancreatic β-cells in a 72 hpf *Tg(ins:Rcamp1.07)* embryo under a wide field microscope.

782

Supplemental Movie 2. Scheme of the dual-colour 2P3A-DSLM and comparison among 1P-SPIM, TPM and 2P3A-DSLM in islet 3D imaging of live zebrafish.

785

Supplemental Movie 3. Representative time-lapse volumetric reconstruction of glucose-stimulated calcium transients in all pancreatic β-cells from 72 hpf *Tg(ins:Rcamp1.07)* embryos observed under the 2P3A-DSLM.

789

Supplemental Movie 4. Volumetric reconstruction of pancreatic β-cells and their nearby blood vessels in living *Tg(ins:EGFP);Tg(flk1:mCherry)* embryos from 36 hpf to 72 hpf.

792

Supplemental Movie 5. Representative time-lapse volumetric reconstruction of glucose-stimulated calcium transients in all pancreatic β-cells from 72 hpf *Tg(ins:Rcamp1.07)* embryos that had been treated with 3-MPA.

796

Supplemental Movie 6. Representative time-lapse volumetric reconstruction of glucose-stimulated calcium transients in all pancreatic β-cells from 72 hpf *Tg(ins:Rcamp1.07)* embryos that had been co-treated with 3-MPA and CGA.

800

801

802

803

804

805

806

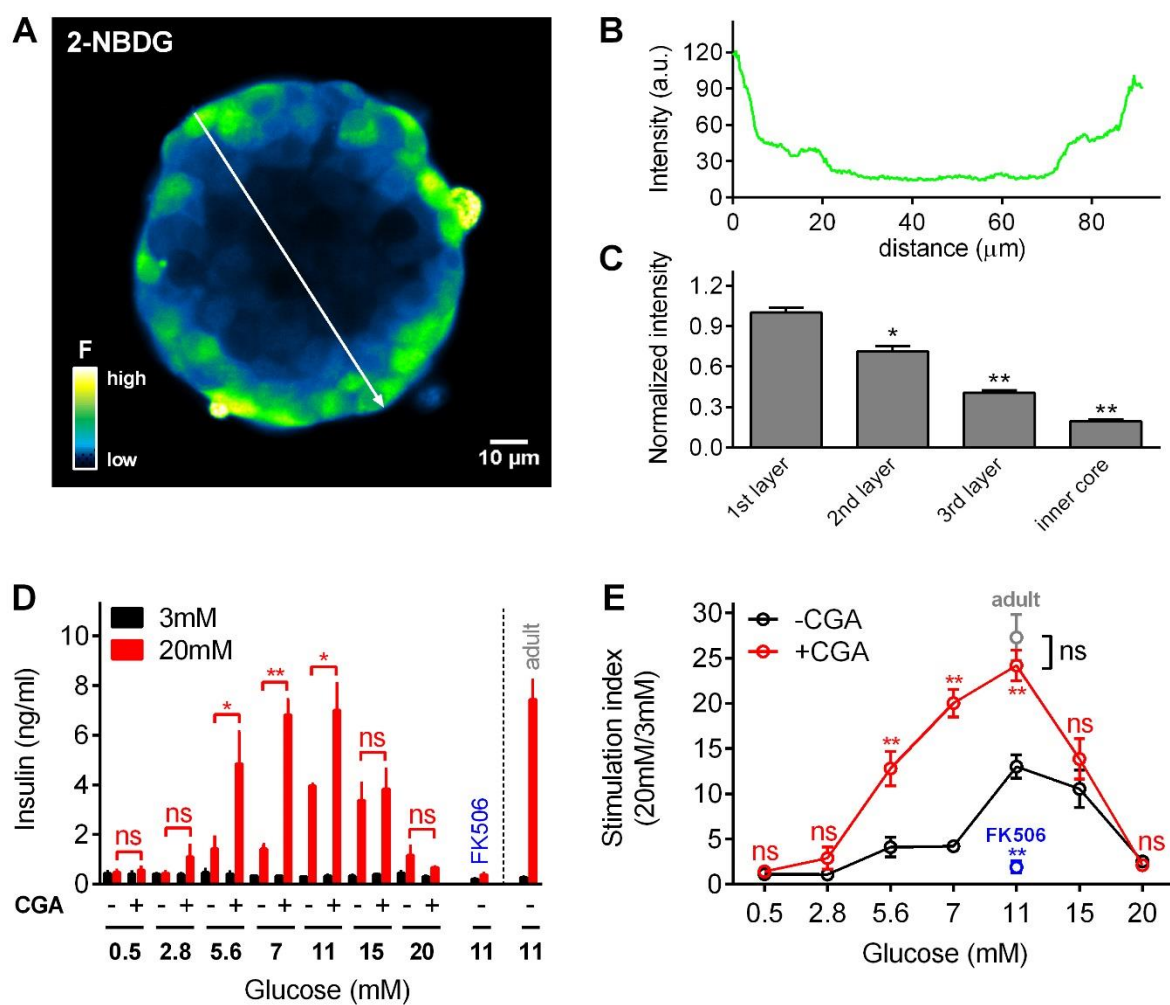807

808

809

810

811

812

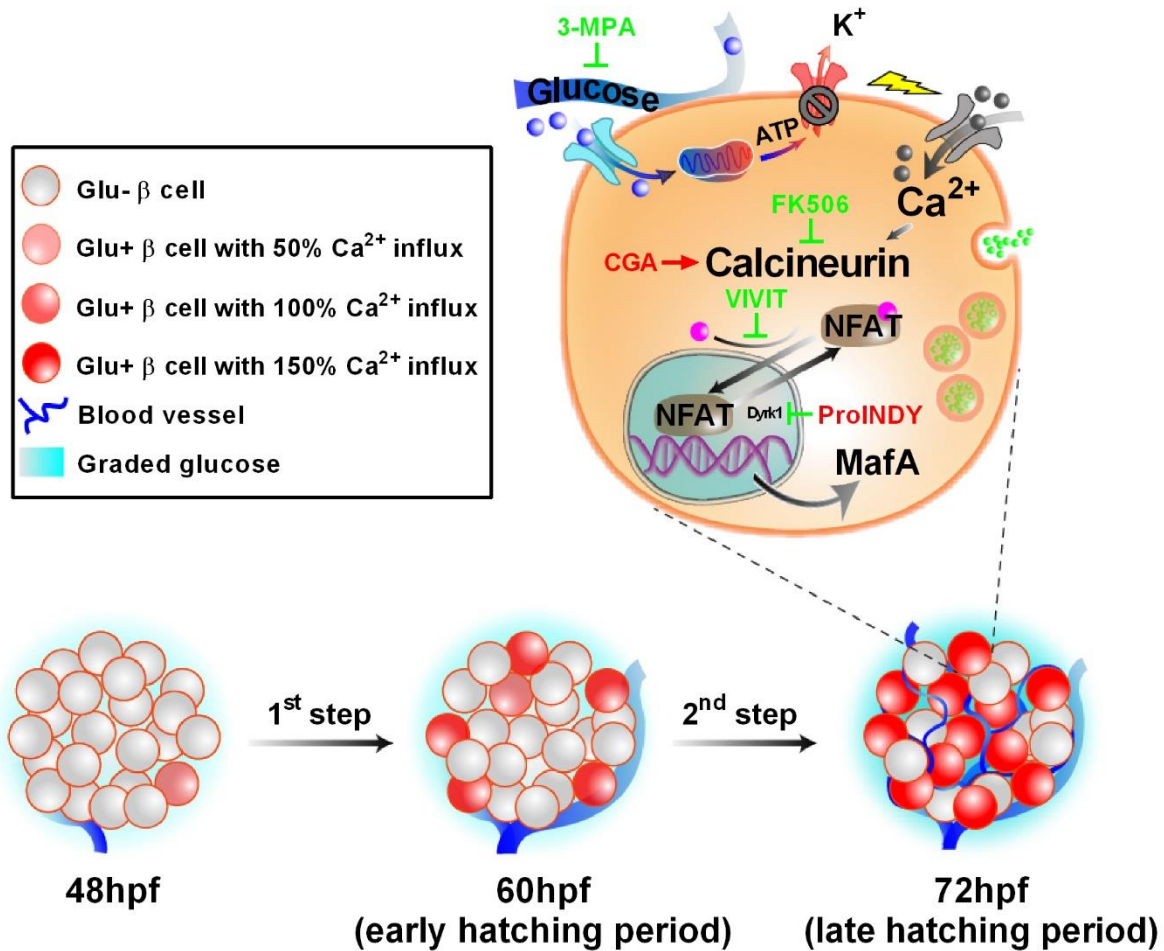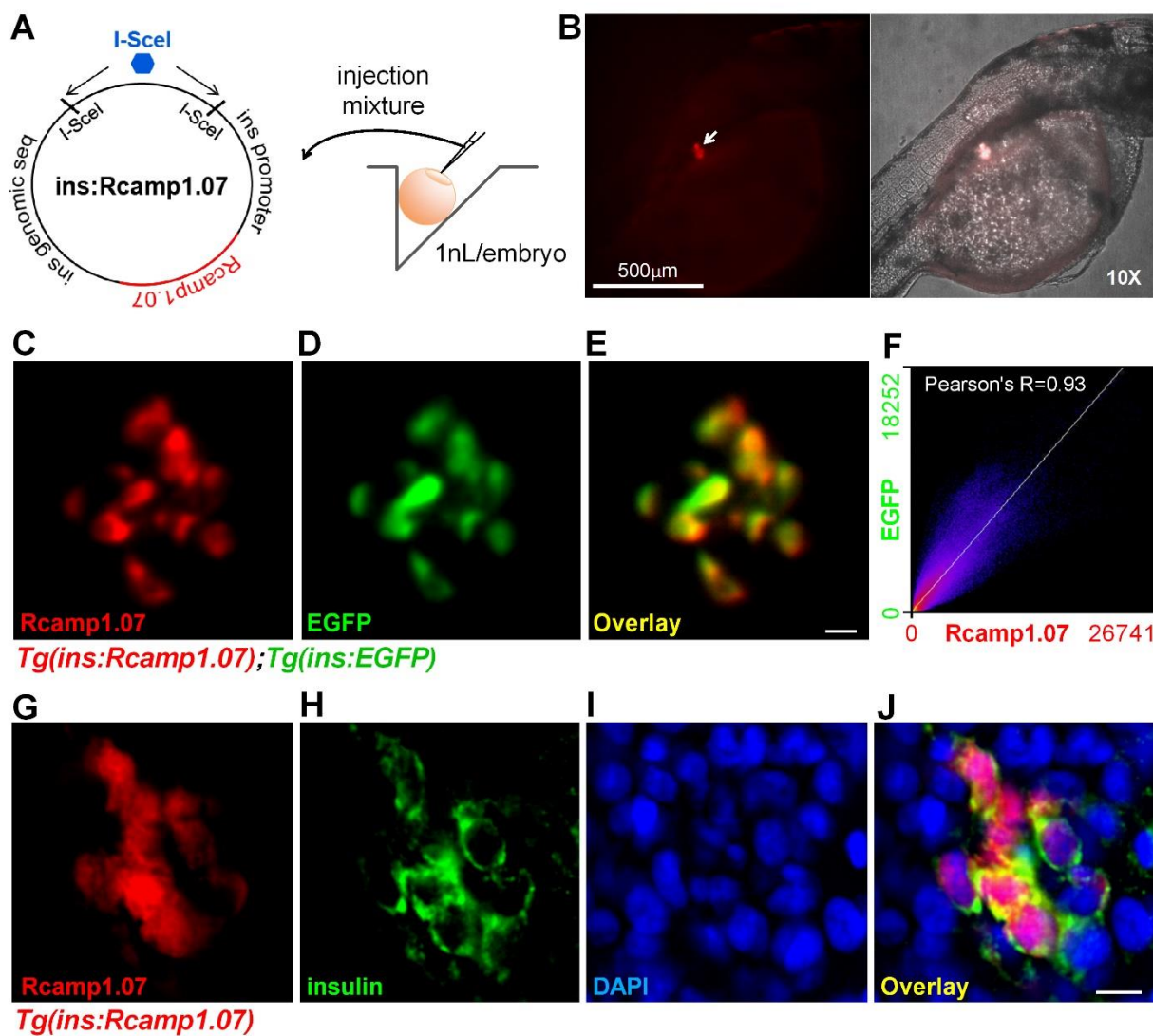813

814

815

816
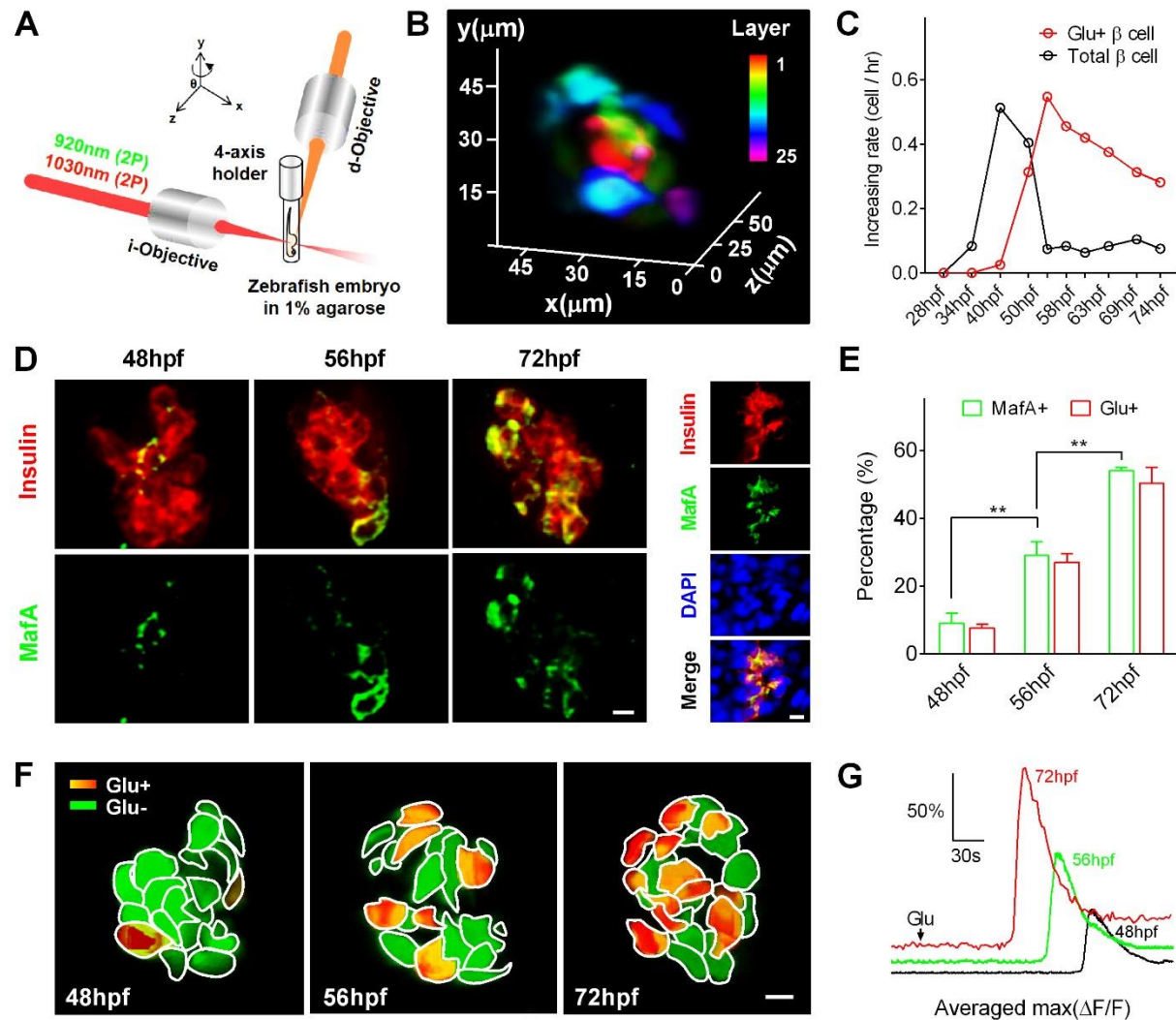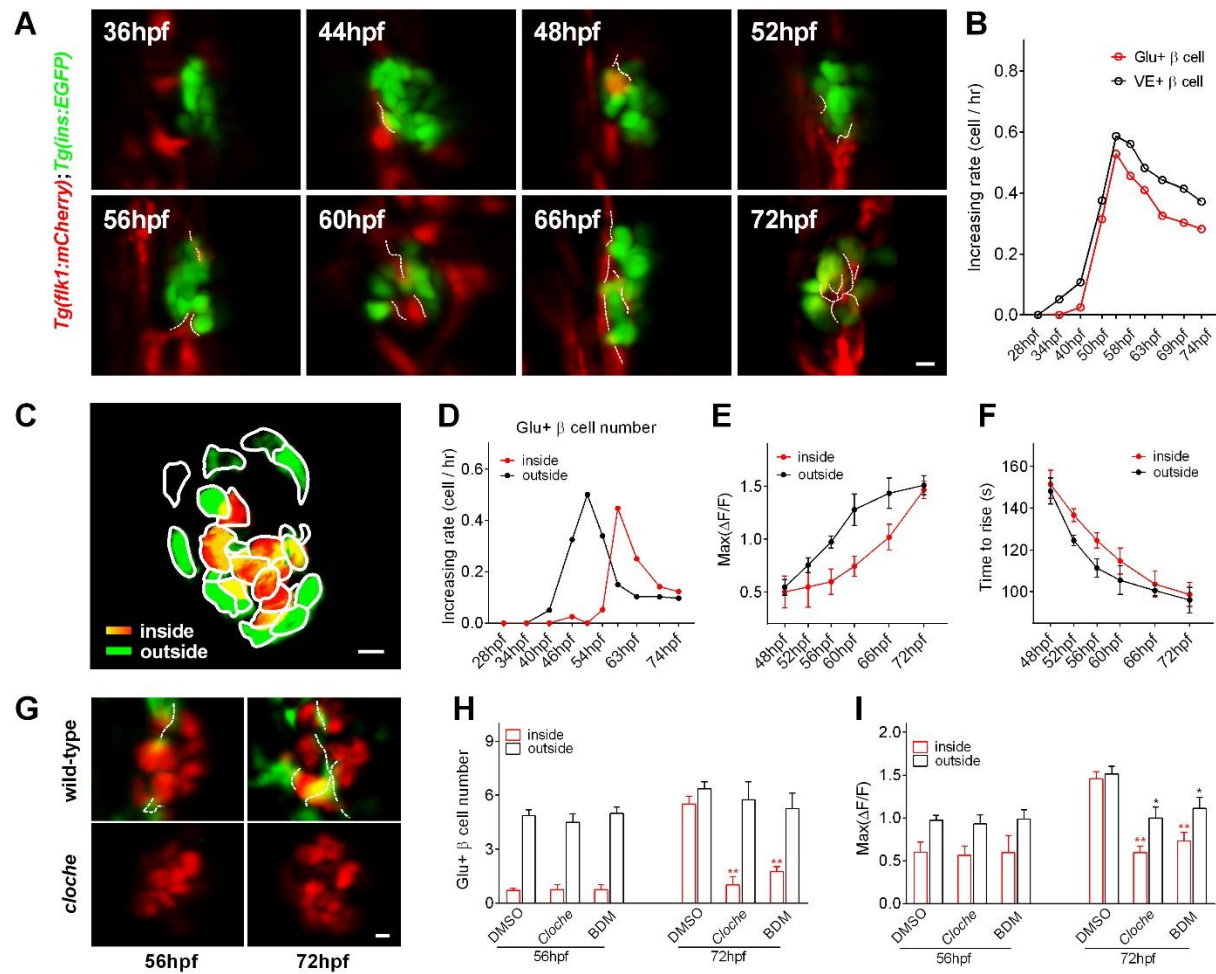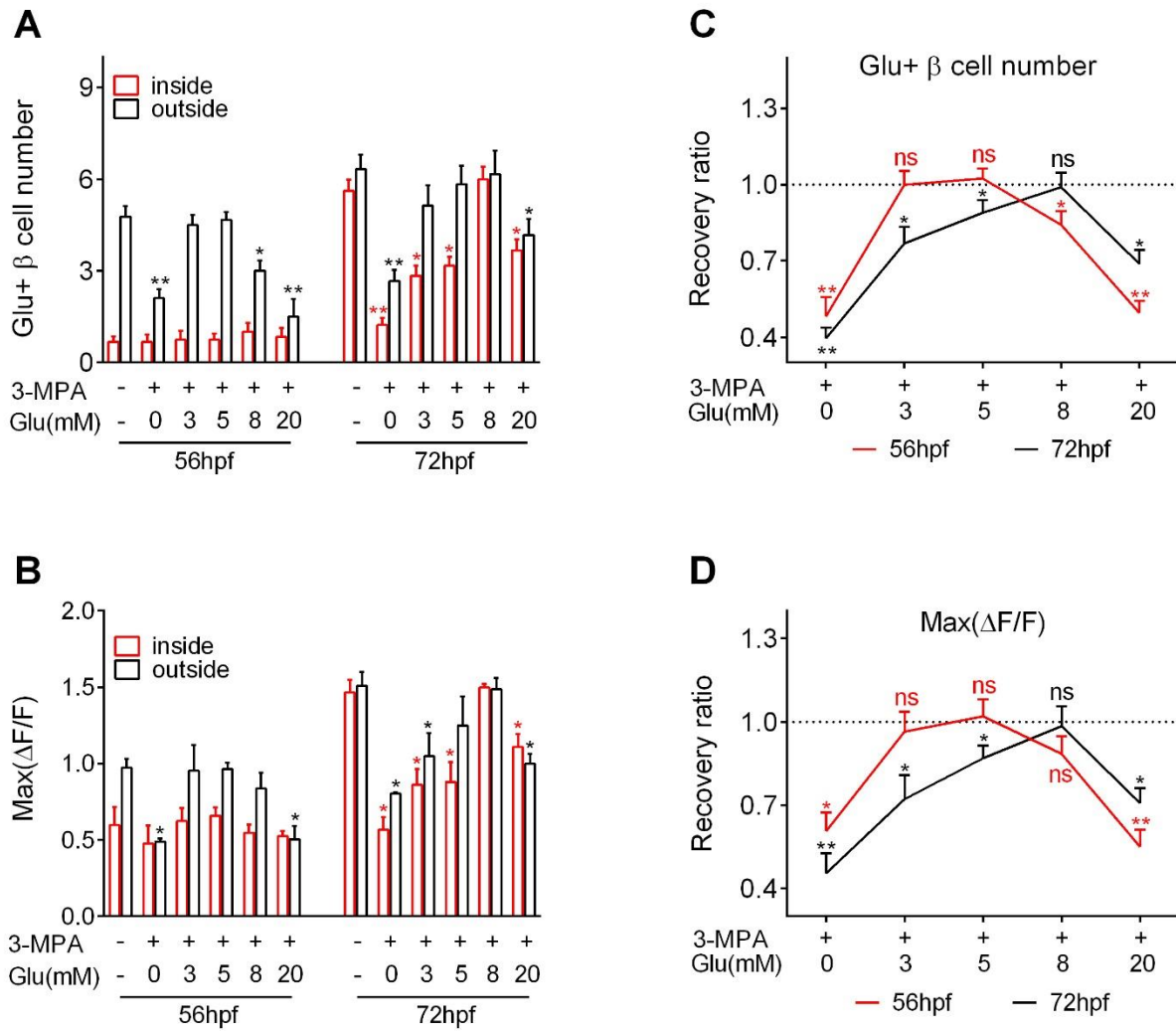
817

818
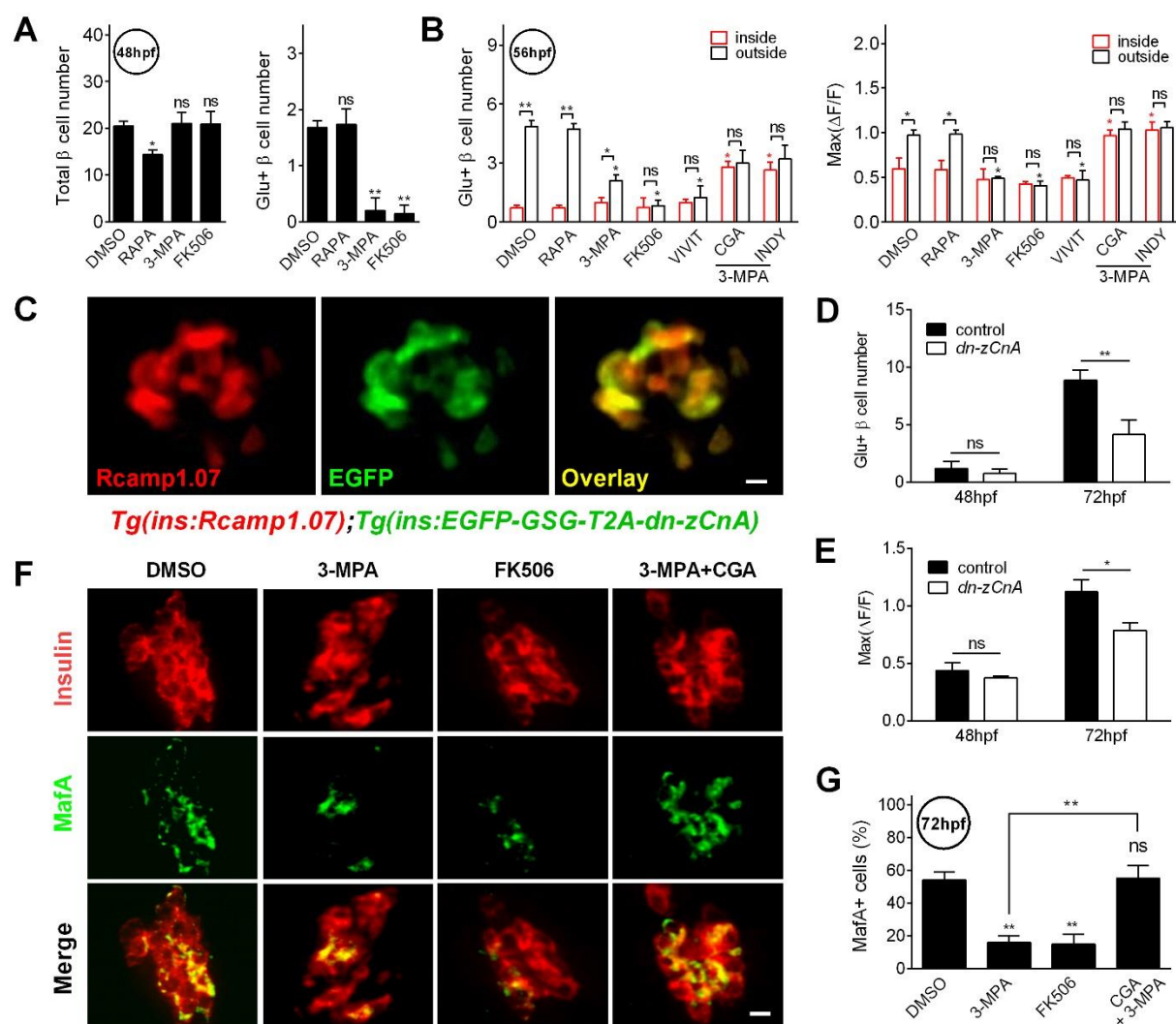
819

820

821

822

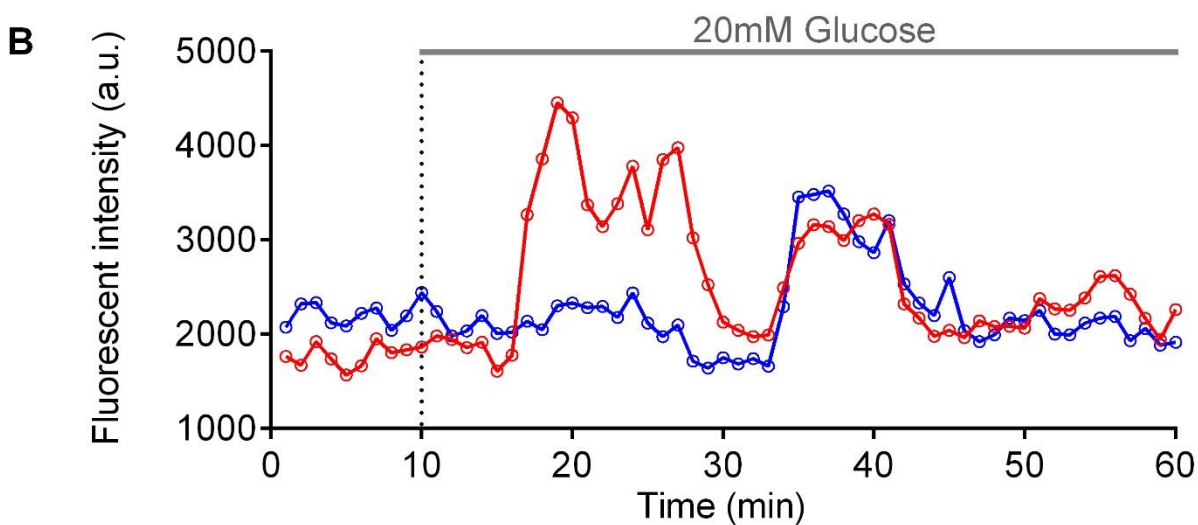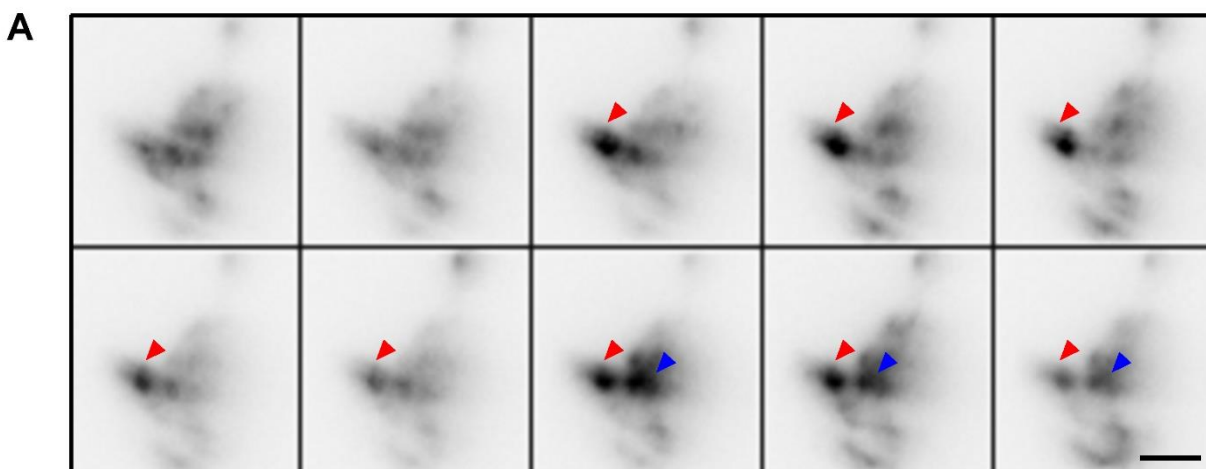# Microcirculation-coordinated, Glucose-triggered, Calcineurin/NFAT-dependent β-cell Maturation *in vivo*

823

824

825

826

827

828
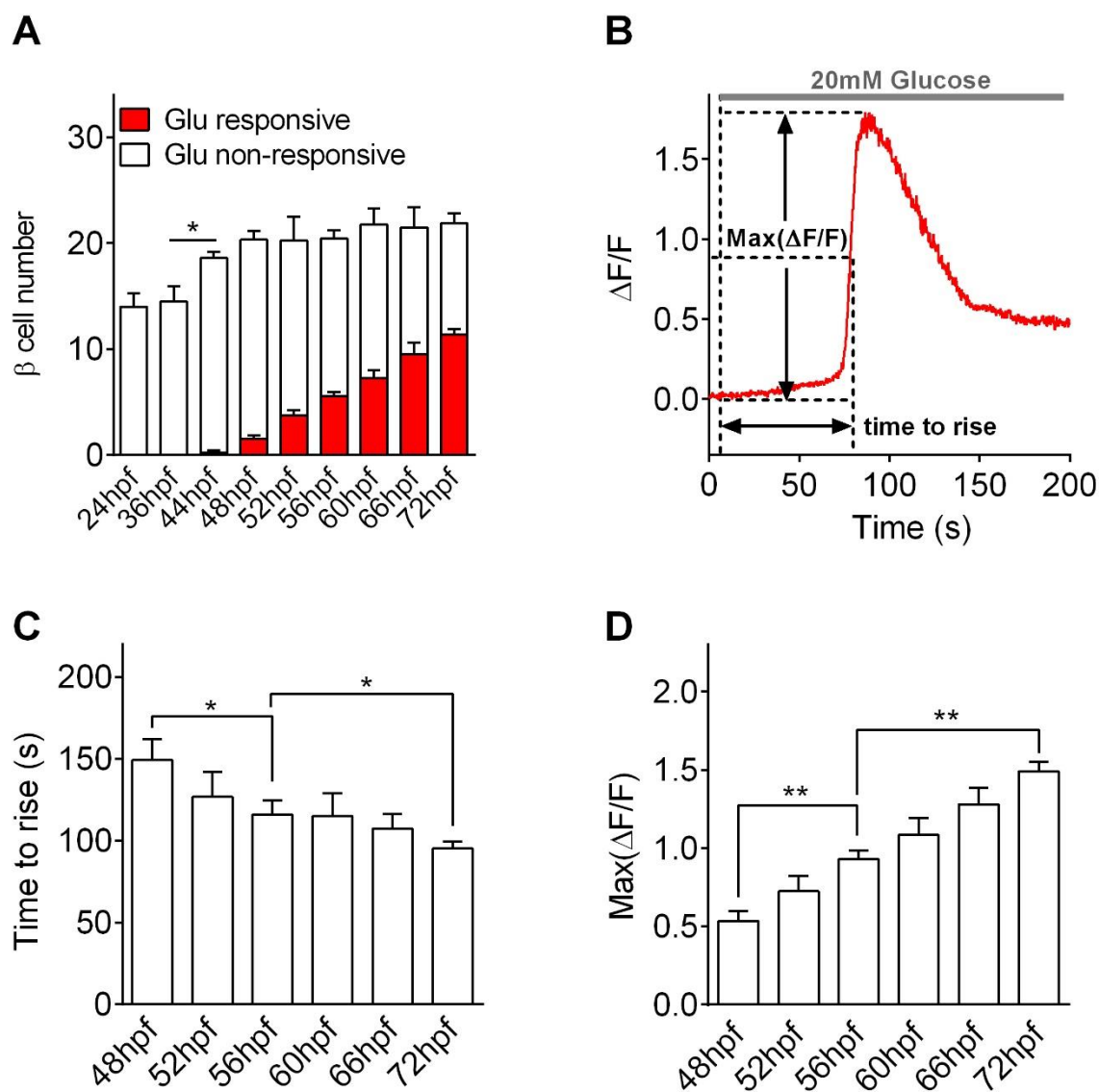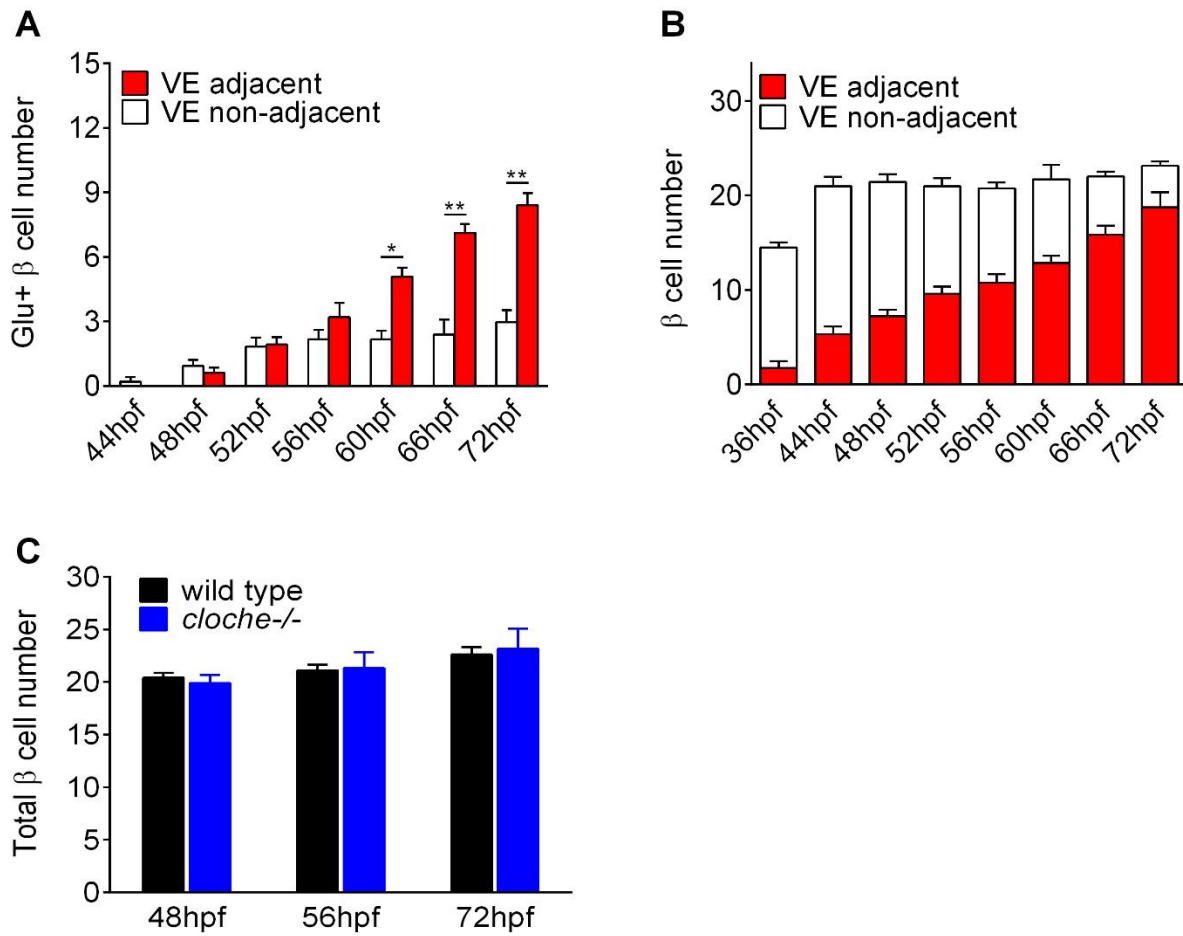
829

830

831

832

833

834

835

836

837

838

839

840

841
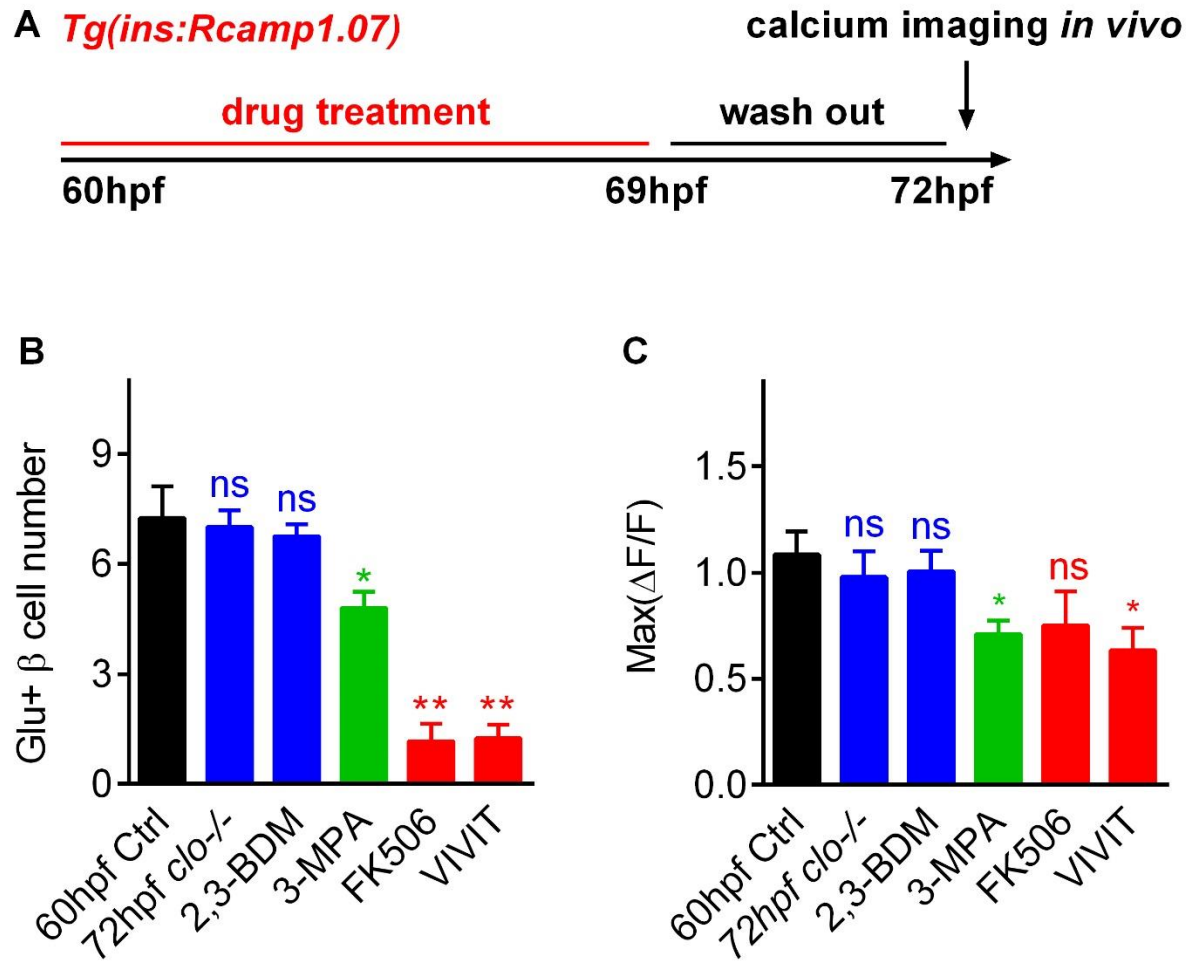
842

843

844

845

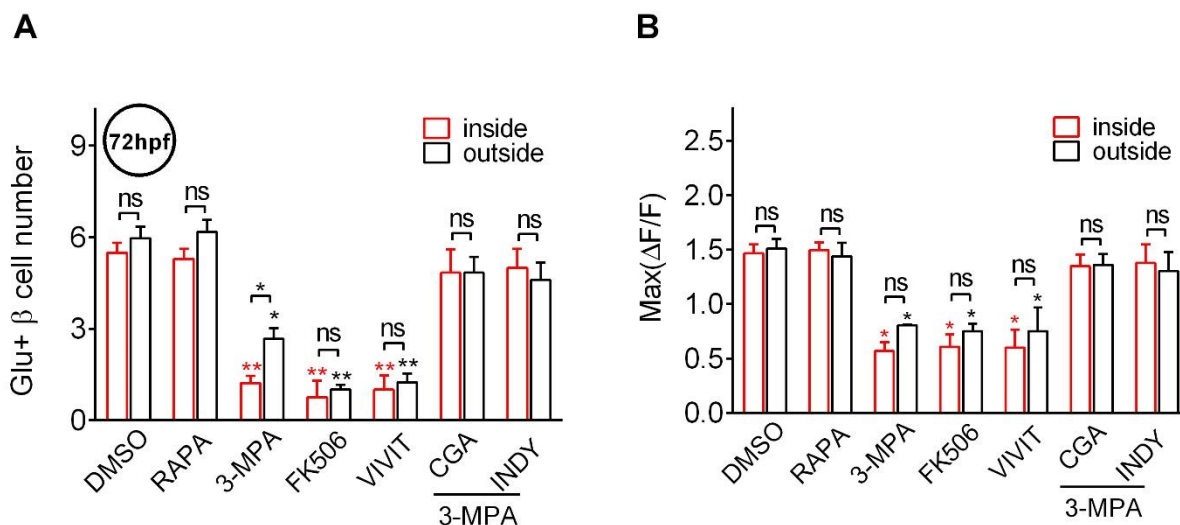846

847

848

849

850

851

852

853

854

Comparison of events and critical time window in zebrafish and mouse pancreas development

Developmental process	Zebrafish		Mouse	
	Events	Stage	Events	Stage
Pancreatic specification	*Pdx-1* appears in pancreatic primordial (Tiso et al, 2009)	10 somite	*Pdx-1* appears in dorsal endoderm (Shih et al, 2013)	E8-E8.5
Pancreatic budding	emergence of *insulin* gene (Tehrani & Lin, 2011; Tiso et al, 2009)	15 somite	dorsal bud appears (Avolio et al, 2013; Nair & Hebrok, 2015) α-cells appear first (Yamaoka & Itakura, 1999)	E8.5-E9.5
	dorsal bud appears (Tehrani & Lin, 2011; Tiso et al, 2009)	24hpf	ventral bud appears (Avolio et al, 2013; Nair & Hebrok, 2015) β-cells and δ–cells appear (Yamaoka & Itakura, 1999)	E9.5-E10.5
	emergence of *glucagon* gene (Tiso et al, 2009)	22-26hpf		
	ventral bud appears (Tehrani & Lin, 2011; Tiso et al, 2009)	32-40hpf		
Rotation and buds fusion	fusion of dorsal bud and ventral bud (Tehrani & Lin, 2011; Tiso et al, 2009) emergence of *ghrelin* and *trypsin* genes (Tehrani & Lin, 2011; Tiso et al, 2009)	48-52hpf	tip and trunk domain formation (Avolio et al, 2013; Zhou et al, 2007) trunk domain has Nkx6.1, Sox9 (Avolio et al, 2013; Zhou et al, 2007) scattered islet aggregates formation (Avolio et al, 2013)	E12.5-E14.5
Islet morphogenesis	complete fusion of the two buds (Tehrani & Lin, 2011; Tiso et al, 2009) principal islet forms core-mantle structure (Tehrani & Lin, 2011; Tiso et al, 2009)	52-72hpf	condense islets form core-mantle structure (Shih et al, 2013)	E18.5-E20
Islet vascularization	initiation with aorta contacting principal islet (Field et al, 2003b) perfusion with blood flow in most vessels fully vascularized principal islet	36-44hpf 48-60hpf 66-72hpf	initiation with endocrine cell differentiation (Reinert et al, 2014; Shah et al, 2011) perfusion with blood flow in most vessels (Shah et al, 2011) completed islet vascularization (Reinert et al, 2014)	E13.5 E14.5 E20-at birth
β-cell differentiation	emergence of insulin-positive cells (Tehrani & Lin, 2011; Tiso et al, 2009) β-cell proliferation (independent of Cn/NFAT) (Tsuji et al, 2014) appearance of glucose-responsive β-cells β-cell functional maturing	15 somite 36-40hpf 44-48hpf 48-72hpf	emergence of insulin-positive cells (Yamaoka & Itakura, 1999) rapid expansion of β-cells (independent of Cn) (Goodyer et al, 2012b; Shah et al, 2011) appearance of glucose-responsive β-cells (Hole et al, 1988; Reinert et al, 2014; Rozzo et al, 2009) β-cell functional maturation (Blum et al, 2012a)	E9.5-E10.5 E14.5 P2 P9

855